KBS TEKNISK RAPPORT 97

Colloid chemical aspects of the »confined bentonite concept»

Jean C Le Bell

Ytkemiska Institutet 1978-03-07

KÄRN - BRÄNSLE - SÄKERHET

POSTADRESS: Kärnbränslesäkerhet, Fack. 102 40 Stockholm. Telefon 08-67 95 40

COLLOID CHEMICAL ASPECTS OF THE "CONFINED BENTONITE CONCEPT"

Jean C Le Bell
Ytkemiska Institutet 1978-03-07

I slutet av rapporten har bifogats en förteckning över av KBS hittills publicerade tekniska rapporter i denna serie.

COLLOID CHEMICAL ASPECTS OF THE "CONFINED BENTONITE CONCEPT"

YTKEMISKA INSTITUTET

YTKEMISKA INSTITUTET

The Swedish Institute for Surface Chemistry
Das Schwedische Institut für Grenzflächenforschung
L'Institut Suedois de la Chimie des Surfaces

Adress: Forskningsstationen i Stockholm Drottning Kristinas väg 45 114 28 STOCKHOLM
Telefon 08/22 25 40 Postgiro 35 49 95-3 Bankgiro 20-1650

COLLOID CHEMICAL ASPECTS OF THE "CONFINED BENTONITE CONCEPT".

Jean C. Le Bell

1978-03-07

Table of contents

1. Summary

A short review of concepts in colloid chemistry of relevance to the investigation is given. The basic principles of coagulation and swelling by electrolytes and swelling pressure are discussed. A survey is given of literature of relevance to the colloid chemical properties of the bentonite to be used as buffer mass for waste cannisters in the final respository.

Measurements of the amount of particles released from a bentonite gel by light scattering and visual inspection show that while particles are released in distilled water, the gel will be coagulated if in contact with ground water and consequently the release of particles is negligibly small.

Studies of sedimentation volumes by ultracentrifugation also clearly indicate that the bentonite in contact with ground water under the repository pressure will form a completely stable coagulated gel.

The swelling of confined bentonite was studied in an "artificial crack" of width 0.5 mm. The bentonite flowed readily into this crack and into the much narrower crack formed when the cell was broken. The swelling properties of the bentonite at the repository depth are discussed. It is argued that the gel, if sufficient volume is available, will swell spontaneously to a volume that is $\approx 30\%$ larger than the initial one and then form a stable, coagulated gel containing 30-35% water in equilibrium with the ground water.

Investigations of the diffusion of colloidal matter (sodium lignosulphonate molecules of mean diameter 6 nm) and calcium ions into a dilute bentonite gel show that colloidal matter very probably will have a negligible rate of diffusion while the calcium ions diffuse rapidly. This implies that the initial bentonite gel which is partially in its sodium form will be completely exchanged to its calcium form when brought into contact with ground water which ensures that it will remain coagulated even in its swollen state.

2. Background

The proposed system for radioactive waste isolation uses a buffer material, highly compacted sodium bentonite, to provide an almost completely impermeable zone around the waste cannisters. It is thought that the swelling caused by the ground water uptake causes the compressed bentonite to fill and seal off any cracks occurring after deposition. Also the diffusion of radionuclides is expected to be very low in the barrier.

When the ground water reaches the buffer material a gradual dilution of the bentonite will take place . Although the ground water flows extremely slowly, a removal of particles from the formed bentonite gel due to diffusion by Brownian motion may be envisaged. The release of particles will be governed by the colloid chemical properties of the gel, i.e. the particle interactions that cause its flocculation or deflocculation. These interactions, in turn, are highly dependent upon the composition of the ground water. It is to be expected that the presence of especially multivalent cations will almost completely determine these properties. The chemistry of the ground water is also of utmost importance for the swelling pressure, as the magnitude of pressure, which can be obtained, almost certainly is determined by the composition of the ground water.

The modes of particle aggregation in the bentonite gel, i.e. "card-house" or "card-pack" structures etc., will also be of importance for the permeability and diffusion properties.

The scope of the present investigation has been, apart from surveying relevant literature, to answer the following questions: a) Is it possible that colloidal particles, which can be carriers of radioactive nuclides, or radioactive material in colloid form, are able to diffuse through the gel? b) Is it to be expected that newly formed cracks are filled with bentonite and thus sealed off? c) Is there a possibility of release of small amounts of buffer material in cracks where the water-swollen bentonite gel is in contact with pure ground water?

3. Concepts in colloid chemistry

3.1 The electrical double layer

At an interface ions and solvent molecules are affected by electrical potential differences between the phases and by the van der Waals forces. This leads to

i) an orientation of the dipoles of the solvent
ii) a structuring of charges in layers parallel to the interface.

This orientation gives rise to electrical gradients at the interface, although the assembly as a whole is electrically neutral. The structure of this so-called electrical double layer is schematically shown in Fig. 3.1,whereas the corresponding variation of the potential with distance from surface in the various regions is shown in Fig. 3.2.

In the case of an interface between a solid surface and a simple electrolyte solution the following model of the charge distribution (the Stern - Guoy - Chapman model) is generally accepted.

The double layer can be divided into the following distinct regions:

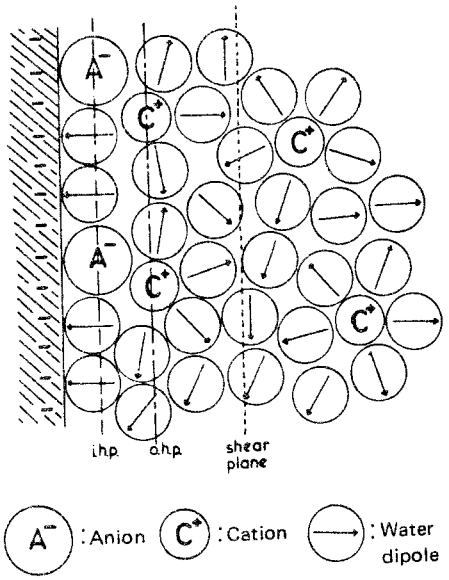

Figure 3.1 *A schematic representation of the electrical double layer.*

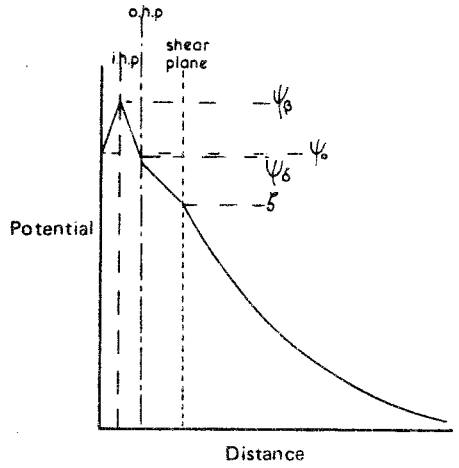

Figure 3.2.*Variation of potential corresponding to Fig.* 3.1.

1. The innermost region adjacent to the interface, contains a layer of specifically adsorbed ions; such ions no longer have their hydration shells intact, and since anions are more easily dehydrated, the innermost layer very often consists of anions, irrespective of the sign of the charge on the interface itself. Water molecules are also always present because of the strong dipolar forces between them and the interface. The plane defining the extent of this layer is for historical reasons called the inner Helmholtz plane (i.h.p.). The potential relative to the electrolyte solution in the i.h.p. is denoted $\psi\ \beta$.

2. Outside the i.h.p. there is a region containing the hydrated counter ions (with opposite charge to the surface). In this region there are also water molecules bound between the hydrated ions. The plane defining the extent of this region is called the outer Helmholtz plane (o.h.p.) with potential $\psi\ \delta$.

3. Outside the o.h.p. there is a layer in which the hydrated ions are moving freely in the solvent, but still are attracted or repelled by electrostatic forces from the interface. This leads to an excess of attracted and a deficiency of repelled ions relative to the neutral electrolyte solution close to the interface. The deviation from neutrality decays gradually (approximately exponentially) at sufficient distance from the surface the thermal motion of the ions dominates and the

solution is neutral. This layer is called the diffuse layer. The thickness of the diffuse layer ($1/\kappa$) is usually defined as the distance from the o.h.p. at which the potential has fallen to $\psi\delta/e$ and is given by

$$\kappa = \left(\frac{2Z^2F^2C_o}{\varepsilon_o \varepsilon_r RT} \right)^{1/2} =$$

where Z = Charge of the counter ions
F = Faraday's constant
C_o = Concentration of electrolyte
ε_r = Relative permittivity of the solvent
ε_o = Permittivity of vacuum
R = The gas constant
T = Temperature

κ is the Debye-Hückel parameter commonly used in electrolyte theory.

The implication of this equation is that the diffuse layer is of importance only in dilute electrolyte solutions (< 0.1 mol dm^{-3}). The decrease in potential with distance is shown in Fig.3.4 and 3.5.

3.2 The Zeta potential and electrophoretic mobility

Experimentally, the double layer surrounding a colloidal particle is often studied by microelectrophoresis, i.e. by measuring the velocity of the particles in solution in an electrical field. This velocity is related to the potential shown by the kinetic unit formed by the particle towards the surrounding solution, the zeta potential. This is usually considered to be the potential in a shear plane outside of the o.h.p. Fig.3.2. The precise location of this plane is a problem which has not been solved with complete satisfaction. For colloidal particles there are a number of complicated corrections which must be applied. However, under favourable conditions, the z-potential gives a rather good estimate of the potential of the particle in the o.h.p.

For large particles the zeta-potential is given by

$$\frac{v}{E} = u_E = \frac{\varepsilon \zeta}{4 \pi \eta}$$

u_E = electrophoretic mobility of the particle
v = velocity of the particle
E = the strength of the applied field
η = viscosity of the dispersion medium
ε = relative permittivity of the dispersion medium
ζ = the zeta-potential

3.3 Colloid stability

Close approach of two particles with surfaces with associated double layers will result in the generation of a repulsive force between the surfaces. Colloid systems are characterized by the extremely large interface which exists between the disperse phase and the dispersion medium. The repulsive force between the surfaces is therefore of primary importance for the resistance to flocculation, which otherwise occurs spontaneously under influence of long range van der Waals attractive forces.

The first comprehensive theory of the general character of the interaction between colloidal particles was developed by Verwey and Overbeek and Derjaguin and Landau (1-3). The basic premise of their theory, the so-called DLVO theory, was that the potential energy of interaction between a pair of particles could be considered to consist of two components:

1. that arising from overlap of the electrical double layers and leading to repulsion, V_R

2. that arising from electromagnetic effects and leading to van der Waals attraction, V_A

The total interaction between the colloidal particles could thus be obtained by the superposition of the double layer and the van der Waals forces:

$$V_T = V_R + V_A$$

In the simple case involving the interaction between the diffuse double layers associated with colloidal flat plates of infinite extent at a fairly large distance from each other and not too high $\psi\delta$, the following equation is obtained:

$$V_T = \frac{64nkT}{\kappa} \left[\exp\ (-\kappa H_o)\right] \left[\frac{\exp\ (Ze_o\psi\delta/2kT)-1}{\exp\ (ze_o\psi\delta/2kT)+1}\right]^2 - \frac{A_H}{12\Pi H_o^{\ 2}}$$

where k = Bolzmann's constant
T = absolute temperature
n = number of ions per cm^3
κ = reciprocal thickness of the diffuse double layer
H_o = distance of separation between plates
z = valency of the counter ion
e_o = electronic charge
$\psi\delta$ = potential of the outer Helmholtz plane
A_H = the Hamaker coefficient which is characteristic of the combination of particle material and solvent in the system

The general features of the curve of potential energy of interaction against the distance of separation between the particle surfaces, H_o , are given in Figure 3.3:

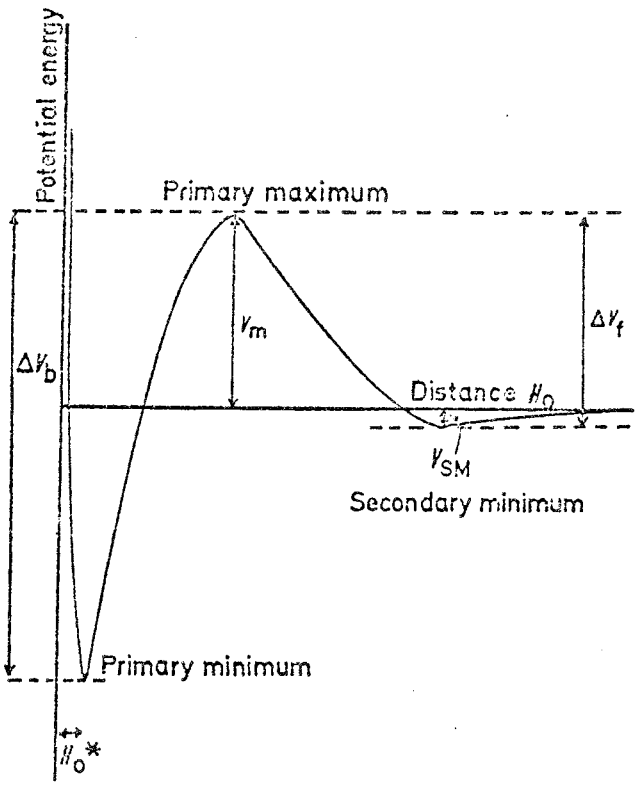

Figure 3.3 *Form of the curve of potential energy* ($V = V_R + V_A$) *against distance of surface separation,* H_0, *for the interaction between two particles (schematic).*

i) At some suitable combination of ionic strength, potential and Hamaker-constant there is a maximum in the potential energy curve. This is normally termed the primary maximum, V_m, and represents the "energy barrier" against coagulation and the magnitude can reach several times the kinetic energy of the particles ($\frac{3}{2}$ kT).

ii) When the particles come closer to each other than the separation which corresponds to the primary maximum, the combination of strong short range repulsive forces and van der Waals attraction leads to a deep minimum, the primary minimum, which determines the distance of closest approach H_0^*.

iii) According to the DLVO theory particles involved in a collision need an excess energy equivalent to the energy barrier to coagulate; usually a colloid is considered stable if the barrier is of the order of 5-10 kT; the kinetic energy barrier to particle association in the primary minimum is represented by ΔV_f

iv) At larger distances, the energy of electrostatical repulsion falls off more rapidly with increasing distance of separation than the van der Waals attraction and a second minimum appears in the curve of depth V_{sm}, the secondary minimum.

v) The energy barrier to redispersion from a primary minimum is represented as ΔV_b.

3.4 Critical Coagulation Concentration (c.c.c.)

If the Hamaker coefficient is known and a fixed value is assigned to ψ_δ, then the variation of the total interaction a) as a function of the concentration of added electrolyte and b) as a function of the valence of the counter ion at constant electrolyte concentration, can be examined. Figures 3.4 and 3.5 show the electrolyte dependence of the potential in the diffuse double layer. It is seen that the potential decreases at an increasing rate as more electrolyte or an electrolyte of higher charge is added.

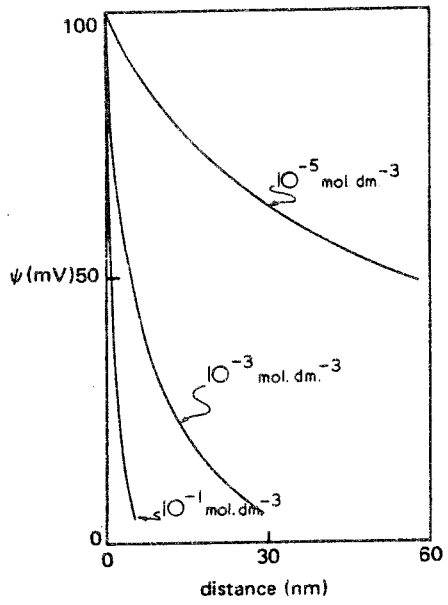

Figure 3.4.*The variation of potential with distance as a function of the concentration of a uni-univalent electrolyte.*

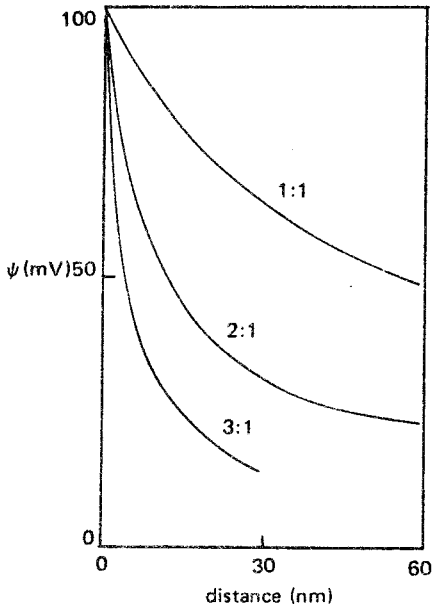

Figure 3.5.*The variation of potential with distance at a constant concentration of* 10^{-5} *mol* dm^{-3} *for a uni-univalent (1:1), a di-univalent (2:1) and a tri-univalent (3:1) electrolyte.*

The form of the potential energy curve (Fig.3.3 gives an explanation for the stability behavior. When the primary maximum has a large positive value ($>$ 5-10kT), then the system is stable, owing to the large activiation energy ΔV_f opposing coagulation. When electrolyte is added, the repulsive forces are decreased due to the effects illustrated in Fig.3.4 and 3.5.

When V_T becomes zero or negative a rapid transition into the primary minimum is faciliated and the system becomes instable, i.e. every collision between particles leads to coagulation. Theoretically the conditions for onset of instability are defined by:

$$V_T = 0$$

$$\frac{\partial V_T}{\partial H_o} = 0$$

From the expressions derived for plate-like particles the electrolyte concentration corresponding to this condition, the critical coagulation concentration (c.c.c.) can be obtained. For T = 298 K,

$$\text{c.c.c.} = \frac{8 \cdot 10^{-22}}{A_H^2 \, Z^6} \text{ mmol dm}^{-3} \quad (\psi\delta > 40 \text{ mV})$$

$$\text{c.c.c.} = \frac{7{\cdot}4 \cdot 10^{-18}}{A_H^2 Z^2} \text{ mmol dm}^{-3} \quad (\psi\delta < 20 \text{ mV})$$

Fig. 3.6 shows the interaction of two parallel plates with variable concentration of 1:1 electrolyte. Increasing concentration of the counterion reduces the height of the repulsive energy barrier until at a particular concentration of electrolyte the potential barrier becomes zero.

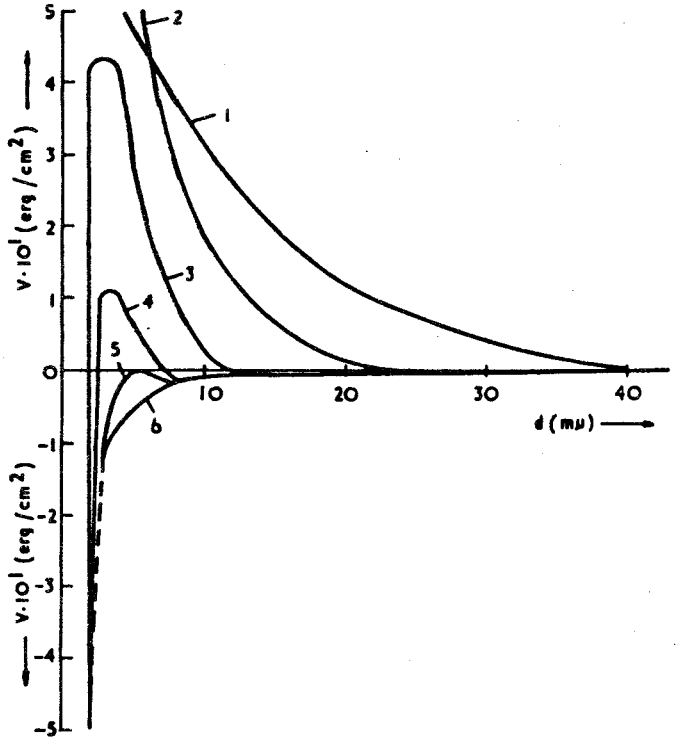

Figure 3.6 *The interaction as a function of interparticle distance for* $A_H = 5x10^{-13}$ *erg,* $\psi_\zeta = 100$ *mV, and variable ionic strength (mol* dm^{-3}*): (1)* 10^{-3}*; (2)* $5x10^{-3}$*; (3)* $2.5x10^{-2}$*; (4)* $5x10^{-2}$*; (5)* $7.5x10^{-2}$*; (6)* $5x10^{-1}$*.*

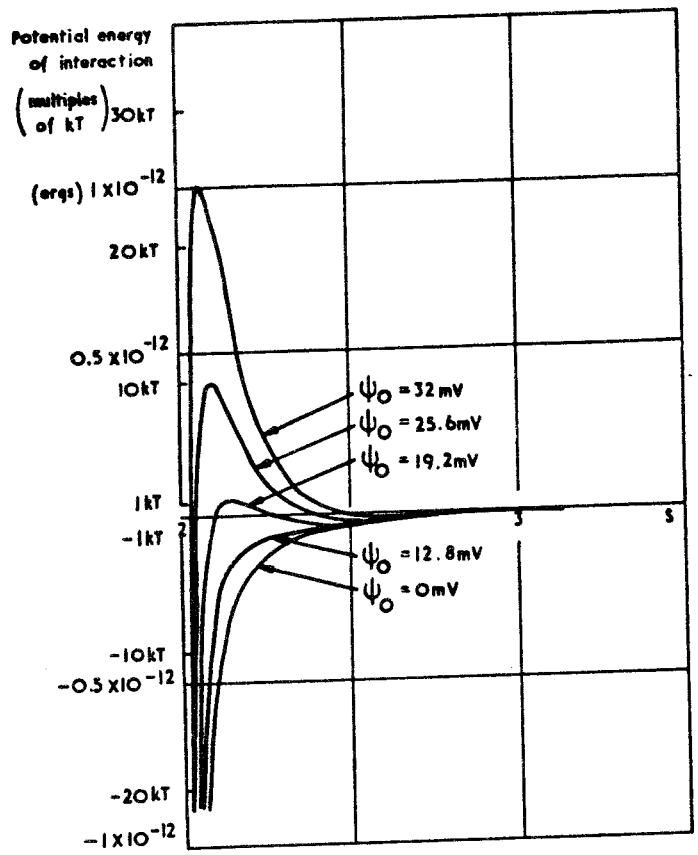

Figure 3.7 The influence of the surface potential ψ_o on the total potential energy of interaction of two spherical particles. Radius = 10^{-5} cm; $A_H = 10^{-12}$ erg;

In fig. 3.7 the interaction energy curve is shown for different surface potentials. Usually a colloid is considered stable when the surface potential is in the range 20-30 mV, corresponding to a zeta-potental $\approx$ 15-25 mV.

At high surface potentials, the coagulation concentration is inversely proportional to the sixth power of the valence of the counter ion, which enables the relative coagulation concentrations of univalent, divalent and trivalent electrolytes to be obtained as

100 : 1.6 : 0.13

which is in good agreement with the empirical relationship from experimental data and known as the Schultze-Hardy rule.

3.5 Swelling pressure

A thin film of liquid sandwiched between two solid phases represents the closest approach to a real system when the behaviour of dispersions are considered from the colloid stability view point, especially for clay platelets. Therefore some aspects on this system will be reviewed.

In a thin film the pressure is not isotropic (hydrostatic), as it is in the interior of the bulk liquid. It should actually be described in terms of a stress tensor. In a planar film the volumetric mean stress, $\bar{p}$, is:

$$\bar{p}^f = \frac{1}{3} (p^N + 2p^T)$$

where p^N is the normal component and p^T the tangential component, and a complete description of the film properties should thus be an equation of state which gives $\bar{p}$ as a function of film composition, thickness and temperature. Usually the properties of the film is described by means of the pressure perpendicular to the film surfaces, i.e. the normal pressure, which is called the "disjoining pressure", Π_D. When the film surfaces are stable at a constant distance from each other, this pressure is zero. Π_D is the difference in chemical potential per unit volume of solvent between the molecules in the thin film and the bulk phase; it is somewhat analogous to an osmotic pressure, where the gradient of chemical potential which arises from a change in chemical composition has to be balanced by a pressure difference.

Interaction forces. In thin films it is more convenient to deal with interaction forces, F, instead of energies:

$$F = \partial V_T / \partial H$$

As the films usually can be considered as planar, the force can be expressed per unit area of film as a pressure:

$$\Pi = F/A$$

A = the area of the film. Corresponding to the potential energies of interaction earlier, the pressures in the film will be:

Π_{el} = electrostatic pressure due to double layer interactions;
Π_{a} = electromagnetic pressure, i.e. van der Waals interactions.
The disjoining pressure will then be:

$$\Pi_D = \Pi_{el} + \Pi_a$$

It perhaps ought to be stressed that this means that, as well as when dealing with colloidal particles, there is, in the case of thin films, a primary maximum on the interaction curve, which opposes the film surfaces to come close to each other under convenient conditions, i.e. there is an equilibrium distance between the surfaces of thin particles, which is dependent on the same variables that are valid for particles in the DLVO-theory, described earlier. This equilibrium distance often corresponds to a high Π_D (several MPa). For a more quantitative treatment of thin films, see Ottewill's article in ref. 3.

4. Properties of Bentonite (montmorillonite) of relevance to its Colloid Chemistry.

4.1 Particle charge and electrokinetic phenomena

Electrokinetic studies of clay suspensions indicate that the c.ay particles carry a net negative charge, above pH values of about 2-3, which is compensated by the presence of cations. One origin of this negative net charge is isomorphous substitution (5), i.e. constituent metal ions of the lattice are replaced isomorphically by cations of lower charge. For montmorillonite chemical analyses show sufficient substitution to account for the observed cation exchange capacity (6, 7). Broken bonds at the adges of the silica-alumina units would also give rise to unsatisfied charges; however, there is evidence that indicates that clay particles carry a positive charge at the edges in acid and neutral media (8-11). Also exposed structural hydroxyls have been suggested to account for the exchange capacity which has recently been discussed (12).

A number of studies indicate that the edges of clay platelets are positively charged at pH values below 6 (13-15). The consequence of oppositely charged edges and faces in aqueous suspensions is a considerable edge-to-face flocculation (6, 9, 10, 16). By addition of various cations or base this structure can be broken down (6, 10, 15). The negative charge on the clay particles is compensated by adsorption of cations. In swelling clays, such as montmorillonite, the cations are adsorbed both on the external surfaces as well as between the unite layers. The cation exchange capacities for montmorillonites are usually in the range 80-100 meq/100 g of clay (7).

In the presence of water the compensating cations have a tendency to diffuse away from the surface since their concentration is smaller in the bulk solution; thus leading to a diffuse double layer. The application of the theory of the diffuse double layer to clay-water systems has not always been successful. Ottewill et al (17) found greater resistance to the reduction of inter layer distance than predicted by the theory, and attributed this to hydration effects; structural boundary layers of water, which must be driven out when decreasing the distance between the clay platelets. Similar suggestions have also been given by Weiss (18), Bolt (19) and Shainberg (20) in taking account the affinity of cations to the clay. van Olphen suggests that face-to-face aggregates are held together by adsorbing clay platelets on the edges of the stacks.

Numerous measurements of the electrokinetic properties are reported. Studies of the influence of various cations and anions as well as the pH on the charge of clays indicate:
i) the negative mobility increases with increasing pH;
ii) anion adsorption has a similar effect;
iii) cations decrease the mobility. The negative mobility changes very little with the concentration of simple cations with low charge but may be reversed by highly charged cations (21, 22). Fig. 4.1-4.4 show the electrophoretic mobility for montmorillonite particles under various conditions (ref. 21, 22. 25, 28 respectively).

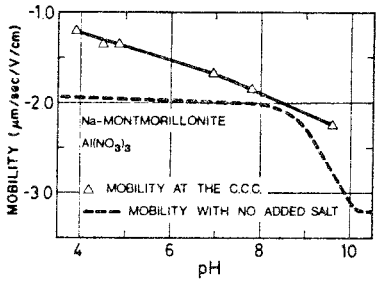

Figure 4.1 *Mobilities of Na-montmorillonite at the c.c.c's of aluminium nitrate (triangles, solid line) and with no salt added (dashed line), as a function of pH.*

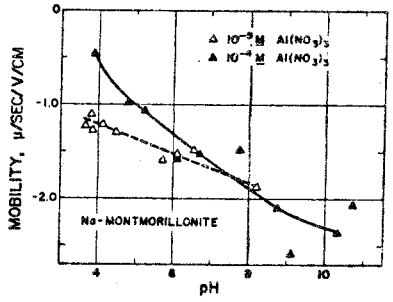

Figure 4.2 *Electrophoretic mobility of Na-montmorillonite as a function of pH, in presence of* $Al(NO_3)_3$. *(Δ):* $[Al(NO_3)_3] = 10^{-5}$ *M, (▲):* $[Al(NO_3)_3] = 10^{-4}$ *M.*

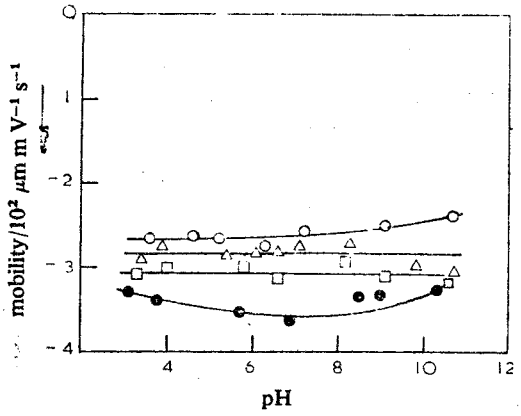

Figure 4.3 *Mobility against pH for sodium montmorillonite particles in various concentrations (mol cm^{-3}) of sodium chloride: -, -, 10^{-4}; -Δ-, 10^{-3}, -0-, 10^{-2}; -●-, 10^{-1}.*

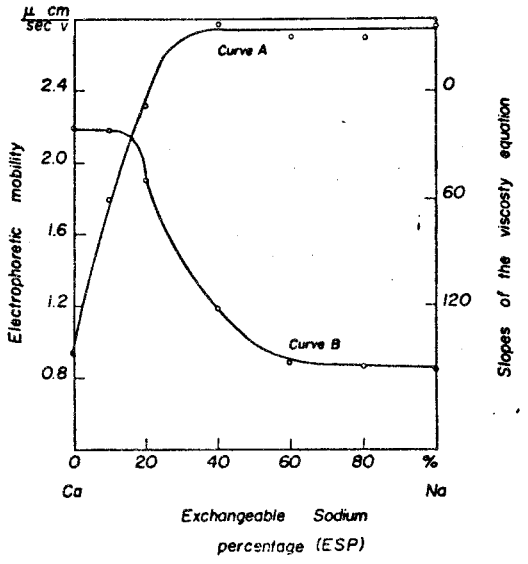

Figure 4.4 *The dependence of electrophoretic mobility (curve A) and the relative size (curve B) of montmorillonite particles on the exchangeable sodium percentage (ESP) [the relative size is expressed in units of the slope in Einstein equation for the viscosity of suspension.]*

4.2 The aggregation of particles in suspensions

When a suspension of clay particles flocculates, association can occur via face-to-face, edge-to-edge and edge-to-face attraction. The electrical interaction energy is governed by three different combinations of the oppositely charged double layers on the faces and edges of the partcles. A variety of structures are possible, depending upon the mode of inter-particle bonding. Some association types for kaolin according to van Olphen (6) are presented in figure 4.5.

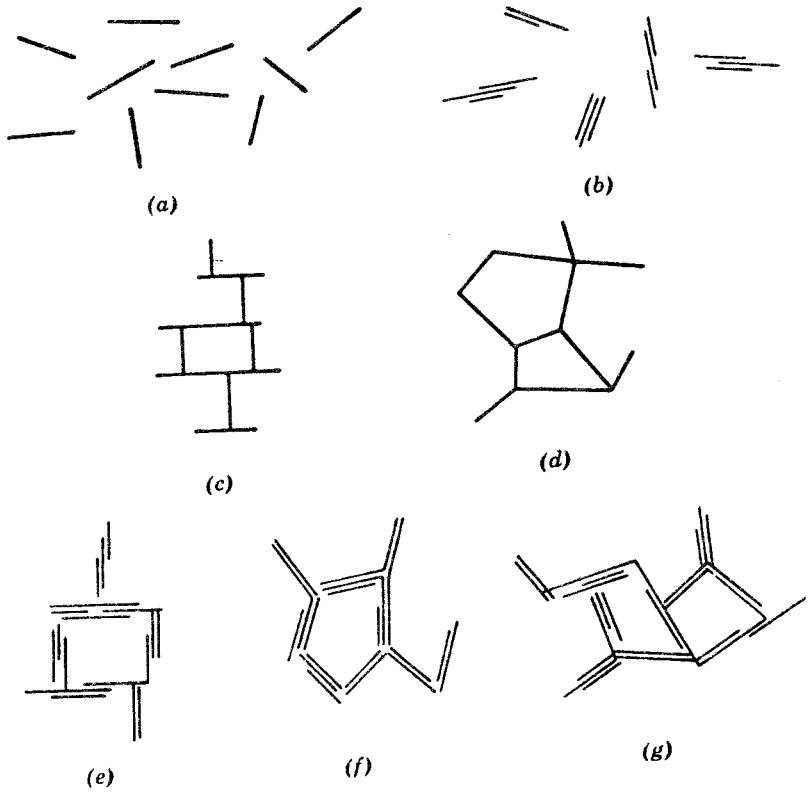

Figure 4.5 *Modes of particle association in clay suspensions, and terminilogy. (a) "Dispersed" and "defloculated". (b) "Aggregated" but "deflocculated" (face-to-face association, or parallel or oriented aggregation). (c) Edge-to-face flocculated but "dispersed". (d) Edge-to-edge flocculated but "dispersed". (e) Edge-to-face flocculated and "aggregated". (f) Edge-to-edge flocculated and "aggregated". (g) Edge-to-face and edge-to-edge flocculated "aggregated".*

In the presence of Ca^{2+} monomorillonite undoubtly forms fact-to-face stacks. These coagulate to form a gel, but whether it is a "card-house" as suggested by van Olphen or a structure determined by "bridging" of the largest particle size fraction of the plates, is still not clear.

Depending on the environment montmorillonite may exist as independent unit layers or as stacks of layers in particles. In general, the amount of face-to-face aggregation decreases and the interlayer spacing increases with decreasing solids concentration, increasing energy of interaction of the interlayer counterions, decreasing electrolyte concentration, and decreasing affinity of the interlayer cations for the clay surface (17, 22-28).

The degree of the different modes of association have been estimated in numerous studies by various techniques including rheological, turbidimetric, microscopic and porosity measurements. van Olphen suggests that deflocculation can be obtained by addition of small amounts of electrolyte thus reducing the edge-to-face attraction by compression of the diffuse double layers; face-to-face and edge-to-edge repulsion is not siffi-ciently decreased to cause this kind of aggregation. If electrolyte is further added to the suspension, the double layers are compressed further, which causes formation of flocs.

4.3 The Stability of Clay Dispersions

The stability of a colloid system can ideally be evaluated from the DLVO-theory. The attractive and repulsive potentials can be calculated and summed as a function of distance of separation between the particles. For coagulation to happen the maxima of repulsion on the total potential interaction curve must not exceed the thermal energy of the particles. The coagulation is usually obtained by reduction of the electrostatic repulsion of the diffuse double layer. This can be accomplished by compressing the double layer by means of adding electrolyte. The higher the valency of the counter ion is, the more efficient is the coagulation.

In clay suspensions the presence of oppositely charged basal and edge surfaces complicates the situation considerably. As mentioned before, a small amount of electrolyte might initally deflocculate the clay, while further addition of electrolyte will coagulate the system. The structure of the coagulated system will be dependent upon the conditions under which the

dispersion was brought to coagulation. The pH will also be of great importance.

In the case of montmorillonite, which has a rather high cation exchange capacity, the coagulation of the clay will be dependent on the preferential order of adsorption of cations, if the coagulating cation differs from the one adsorbed on the clay. The expected dependence upon the charge of the cation, predicted by the DLVO-theory, has been clearly demonstrated (21, 29). The same conclusions are also to be drawn from electrophoretic data (22, 28). For cations of the same charge the ability to coagulate clay suspensions increases with increasing preference for ion exchange of the clay with the cation (21). Some typical critical coagulation concentrations are listed below in table 4.1

Table 4.1

Critical coagulation concentrations (ccc) of sodium and calcium ions for sodium and calcium montmorillonite (mmol dm^{-3})

	Swartzen-Allen and Matijevic (22)	Kahn (29)	Williams and Drover (30)	van Olphen (6)
ccc of Na^+ for sodium montmorillonite	3.5	2	4	12-16
ccc of Ca^{2+} for sodium montmorillonite	0.13	0.1-0.2		1.2-1.3.
ccc of Na^+ for calcium montmorillonite				1,0-1,3.
ccc of Ca^{2+} for calcium montmorillonite				0.08-0.12

The ccc values of ref 6 seem somethat high compared with the other values. However, the value of ccc of Ca^{2+} for sodium montmorillonite is not comparable because it also contains the calcium used for ion exchange; the value of ccc for Ca^{2+} for calcium montmorillonite gives the correct value. However, the critical coagulation concentrations may be quite sensitive to the source of the material and its pretreatment before the experiment.

The amount of face-to-face aggregation increases, in general, with increasing charge of the counter ion, thus resulting in decreased colloidal stability.

The stability dependence on pH often reflects the effect of pH on the coagulant itself, rather than on the clay. Generally the stability is increased with increasing pH; the edge-to-face structure is broken up. If the counter ions are hydrolysed the stability is dependent upon on the complexes present. Data from ref 22 of the pH-dependence are given in figure 4.6.

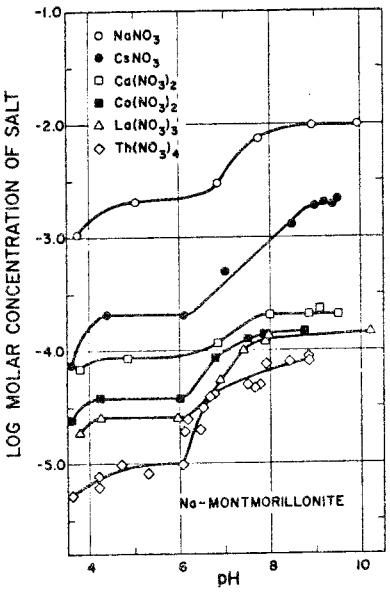

Figure 4.6 *Critical coagulation concentrations of various electrolytes as a function of pH, for a Na-montmorillonite sol (250 ppm). Coagulation occurs under conditions above the lines. Symbols:* ●, $NaNO_3$; □, $Ca(NO_3)_2$; ■, $Co(NO_3)_2$; Δ, $La(NO_3)_3$; ◇, $Th(NO_3)_4$.

4.4 The swelling pressure of montmorillonite

The large increases in volume of montmorillonite in contact with water has been the object of numerous studies. The principles of spontaneous swelling have been discussed by van Olphen (31). In compacted clays there will be a tendency for the plates to become aligned in a parallel fashion. If the clay has a tendency to swell at a certain particle distance (or water content), a net repulsive force exists between the plates. The magnitude of this swelling pressure (or repulsive force) can be measured by applying a confining pressure which will keep the particles at a given distance. Experimental studies have been published by Bolt and Miller (32), Warkentin, Bolt and Miller (33), Warkentin and Schofield (25), Ottewill et al (17,34) and others (22, 36).

According to van Olphen (6) two different situations must be considered. The first one is obtained when the plates are very close together and implies hydration of the dry clay particles when water is adsorbed in successive monolayers on the surfaces. The principal force then is due to the adsorption energy of water layers on the clay surface. The hydration of clays has been treated comprehensively by Forslind and Jacobsson (12). The confining pressure at these short separations has been calculated by van Olphen (37).

The second stage of swelling is due to double layer repulsion which may push the particles further apart. The double layer repulsion can be considered as an osmotic effect usually called osmotic swelling. The discrepancy between the calculated pressure and the measured could be an effect of pressure of non-parallel particles (6) but is probably due to the onset of hydration effects (17). The volume changes due to "osmotic swelling" may amount to as much as a factor 100 with reference to dry clay.

Studies of the interparticle forces in montmorillonite gels (17, 35) indicates reversibility of the system on successive compression and decompression. The observed pressures were always higher for the first compression than for subsequent compression - decompression cycles. This effect was attributed to grain pressure due to edge-face contacts. At higher pressures the plates were thought to re-align to a parallel arrangement.

Increasing the electrolyte content, and consequently compressing the electrical double layer, reduces the swelling pressure considerably. The particles are thus pushed much closer together before the same repulsive force is experienced as at lower electrolyte concentrations.

Data of compressing studies from different investigations are presented in the results part of this report (see fig. 6.6.). It is notable that the swelling ability at high pressures is rather low for higher electrolyte concentrations, especially when the counter ion is divalent.

4.5 Diffusion

Ion movement in clay-water systems has been the subject of several investigations. In many cases the studies have been restricted to systems of very low hydration (38, 39). Diffusional transport was found to occur even in oven-dried clay systems in which the transport must be restricted to counter-ions adsorbed to the clay surface. Studies of highly hydrated systems have been less numerous mainly due to:

i) experimental difficulties, ii) difficulties in the defining of the counterions present in the surface phase. Dufey et al (40, 41) have studied the self-diffusion of anions in clay gels and also sodium influenced by other alkali cations. They found that an increase in electrolyte content and a decrease in porosity yields lateral aggregation of clay particles which increases the path of diffusing anions. For the self-diffusion

of sodium ions in mixed rubidium-sodium clay suspensions the low hydration energy of Rb^+, replacing sodium ions in the vicinity of the clay surface, presumably releases more water molecules to participate in the hydration shell of the sodium ions, thus increasing the surface mobility of sodium ions.

Diffusion of different cations in montmorillonite has been measured by Turk (42) using a conductivity method. The results could be correlated to theoretical calculations of the diffusivity by taking account of ion adsorption and the porosity of the systems. Table 4.2 gives some values for diffusion coefficients of different cations in montmorillonite, taken from ref 39.

Table 4.2

Diffusion coefficients for montmorillonite at different water contents.

% water	4,82	7,30	13,10	19,4
D cm^2 sec^{-1}	$8,88 \cdot 10^{-9}$	$1,96 \cdot 10^{-8}$	$2,64 \cdot 10^{-7}$	$8,83 \cdot 10^{-7}$

Cation	% montm.	D cm^2 $sec^{-1} \cdot 10^7$
Na+	15,2	3,60 ± 0.07
Cs+	16,6	0,40
Ca++	17,9	2,36 ± 0,07
Na	3	3,39 ± 0,19
K	3	4,46 ± 0,28
Ca	3	0,607 ± 0,045
Ba	3	0,358 ± 0,018
Sr	3	0,674 ± 0,040

5. Experimental

5.1 Materials

The bentonite ("Sodium montmorillonite") sample used for the investigations was MX-80 grade. According to the supplier (43), it has a specific gravity of 2.7 g/cm^3 and the pH of water suspensions is in the range 8.5-10. Results from leaching experiments have yielded a pH of ca 9.0 for MX-80 in contact with water at room temperature; at higher temperatures there is a decrease in the pH-values (44).

Cation Exchange Capacity (CEC)

The average exchangable cations for MX-80 are (43)

Element	Meq/100 g
Na+	60-65
Ca++	15-20
Mg++	5-10
K+	1-5

For this particular sample the total CEC was determined to 81.7 meq/100 g (ammonium acetate method) and the sum of magnesium and calcium (Mg+Ca) to be about 55-60 meq/100 g and sodium (Na) about 20-40 meq/100 g (45). Thus the sample used was not a pure sodium montmorillonite. The sample was used as such without any purification nor fractionation.

Synthetic ground water

The composition of the water used is given in table 1 in appendix 1 (46). The water composition is based on analysis of the ground water in the areas suggested for the nuclear waste diposal, and represents the probable average analysis of the ground water (44) (table 2 appendix 1). The ions of importance from a colloid chemical point of view are the cations and especially the multivalent ones. The possible ranges of variation according to ref 44 are given in table 5.1

Table 5.1.

Variations of cation concentrations in ground water (44)

Ca^{2+}	20-40 mg/l	max. 100 mg/l
Mg^{2+}	15-30 "-	150 "-
Na^{+}	20-40 "-	200 "-
Fe_{tot}	1-20 "-	30 "-
Fe^{2+}	0.5-15 "-	30 "-
Mn^{2+}	0.1-0.5 "-	3 "-

In the case of Fe (II) the synthetic ground water is not representative, because the conditions used in these experiments are not reducing as they will be in the real environment. The pH is estimated to be in the range 6.5 - 9.0.

5.2 Diffusion of particles from a bentonite gel

To study the bentonite particles released from a gel the quasi-elastic light-scattering technique was used. The principle of this nethod is that using a laser it is possible to obtain such a high light intensity that a sufficiently small solution volume can be studied to record the fluctuations in scattering intensity due to the brownian motion of the particles. These fluctuations can be related to the particle number and size.

The gel was 15% bentonite (MX-80) in distilled water in contact with water of various compositions (see table 5.2.). The gel was put into test tubes and a sharp flat surface was formed by shearing off the excess bentonite gel. The tubes were then immersed in the water solutions.

The intensity of the scattered light was recorded as a function of time and distance above the gel surface. The method allows determination of the particle concentration in a volume of approx. 10^{-3} mm^3. Hence, the concentrations at 1,2,3,4 and 5 mm from the surface could easily be detected and resolved. The calculation of particle concentrations is described in appendix 2.

Table 5.2.

Water compositions used in light-scattering experiments.

1. Distilled water
2. Calcium cloride, 10^{-4} M
3. -"- 10^{-3} M
4. Synthetic ground water

5.3 Stability of bentonite gels

The release of particles from bentonite gels due to sedimentation was followed by immersing test tubes containing 15% bentonite in water, with their open end downwards. The behaviour of the gels as a function of the calcium chloride content in the water (as well as synthetic ground water and distilled water) and time was recorded.

5.4 Swelling

For the swelling experiment a special cell was used. It consisted of glass plates mounted in a metal frame. Between the glass plates a spacer of 0.5 mm thickness was placed in order to obtain an "artificial crack" of this width. This "crack" was connected to a cavity of 20x40 mm with a thickness of 3.2 mm where a sample of compacted bentonite was placed, figure 5.1. The water, synthetic ground water, could only enter the cell through the "crack". The whole cell was immersed in synthetic ground water and the swelling of the bentonite was recorded as function of the time.

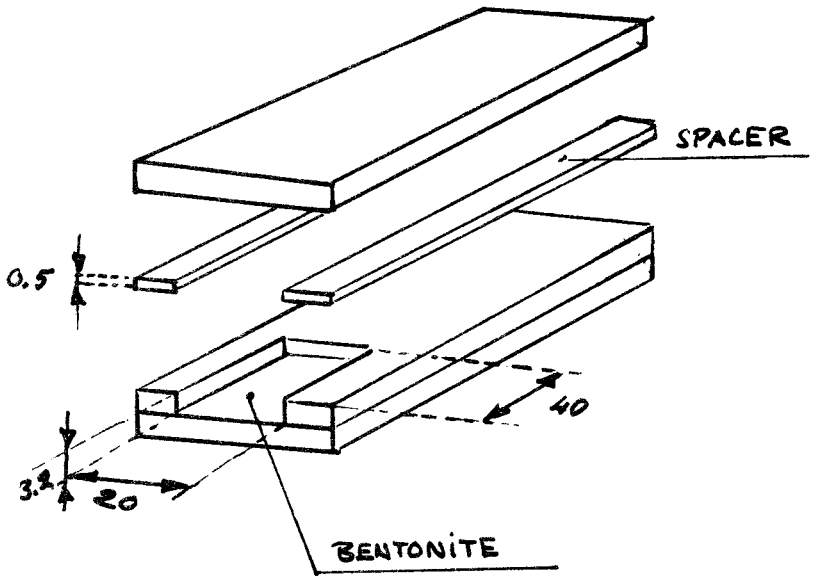

Figure 5.1
Cell for bentonite swelling

5.5 Ultracentrifugation

Measurments of the sediment volume of bentonite suspensions at different concentrations and at different speeds were performed as a function of the water composition. The suspensions were made by dispersing the appropriate amount of dry bentonite in solitions of varying composition. The suspensions were left to equilibriate for two days, after which they were centrifuged. The height of the sediment was measured relative to the initial volume of the suspension.

5.6 Diffusion studies

The diffusion of sodium lignosulphonate (LS) in bentonite gel was studied by keeping a gel in a test tube in contact with a solution containing 240 mg dm^{-3} of a well characterized sample of LS. The mean molecular weight of the LS was 24000, which corresponds to a molecular diameter of about 6 nm &47, 48). The gel in the test tube was then analysed for LS by suspending samples from various depths into 10^{-4} M sodium hydroxide, to desorb the LS from the clay. The concentration of LS was then determined spectrophotometrically at the wave length 280 mm.

The diffusion of Ca-ions in bentonite gel was determined by following the colour change zone, due to cation exchange, advancing in test tubes as a function of time. The bentonite used had a brownish colour, which changes to light-gray when the clay is exchanged to the calcium form. The average distance tube was estimated visually. The concentration of calcium chloride in the solution in contact with the bentonite gel was 10^{-2} M. The evaluation of the results is described in appendix 2.

6. Results and discussion

6.1 Release of particles from the gel

The possibility that bentonite particles might work loose from the buffer mass due to diffusion of particles into the ground water from the gel interface can be evaulated from the light scattering experiments. From the discussion in 4.3, it is obvious that the concentration of, above all, bivalent cations in the ground water will be of extremely large importance for this process. The primary light scattering results for the different aqueous solutions studied are collected in the appendix, figs. 1-7. Figs. 6.1 - 6.4 show the calculated particle concentration as a function of the distance from the gel surface. The following features of these curves should be noted.

1. In the distilled water there is a continued release of particles. The particle concentration at 5 mm distance from the surface rises continuously and is ~ 1 mg dm^{-3} after about 14 days.

2. With increasing concentration of Ca^{2+} the release follows a similar pattern but is much smaller. Thus, after 14 days, the particle concentration in 10^{-4} mol dm^{-3} $CaCl_2$ 5 mm from the surface is also ~ 1 mg dm^{-3}, but in 10^{-3} mol dm^{-3} $CaCl_2$ it is only 0.01 mg dm^{-3}. The diffusion coefficient of the bentonite particles calculated from these measurements is about $2 \cdot 10^{-12}$ m^2 s^{-1}.

3. In synthetic ground water the concentrations at 1 mm distance after 14 days are 10-100 µg dm^{-3}. The conc. at 5 mm distance is so low that the intensity of the scattered light is of the same order as the background intensity, i.e. almost no particles could be detected (cf. appendix, fig. 7). The diffusion coefficient of possibly released particles is $< 5 \cdot 10^{-13}$ m^2 s^{-1}, their size being approximately twice as large in the other waters. That there is an order-of-magnitude

Fig. 6.1

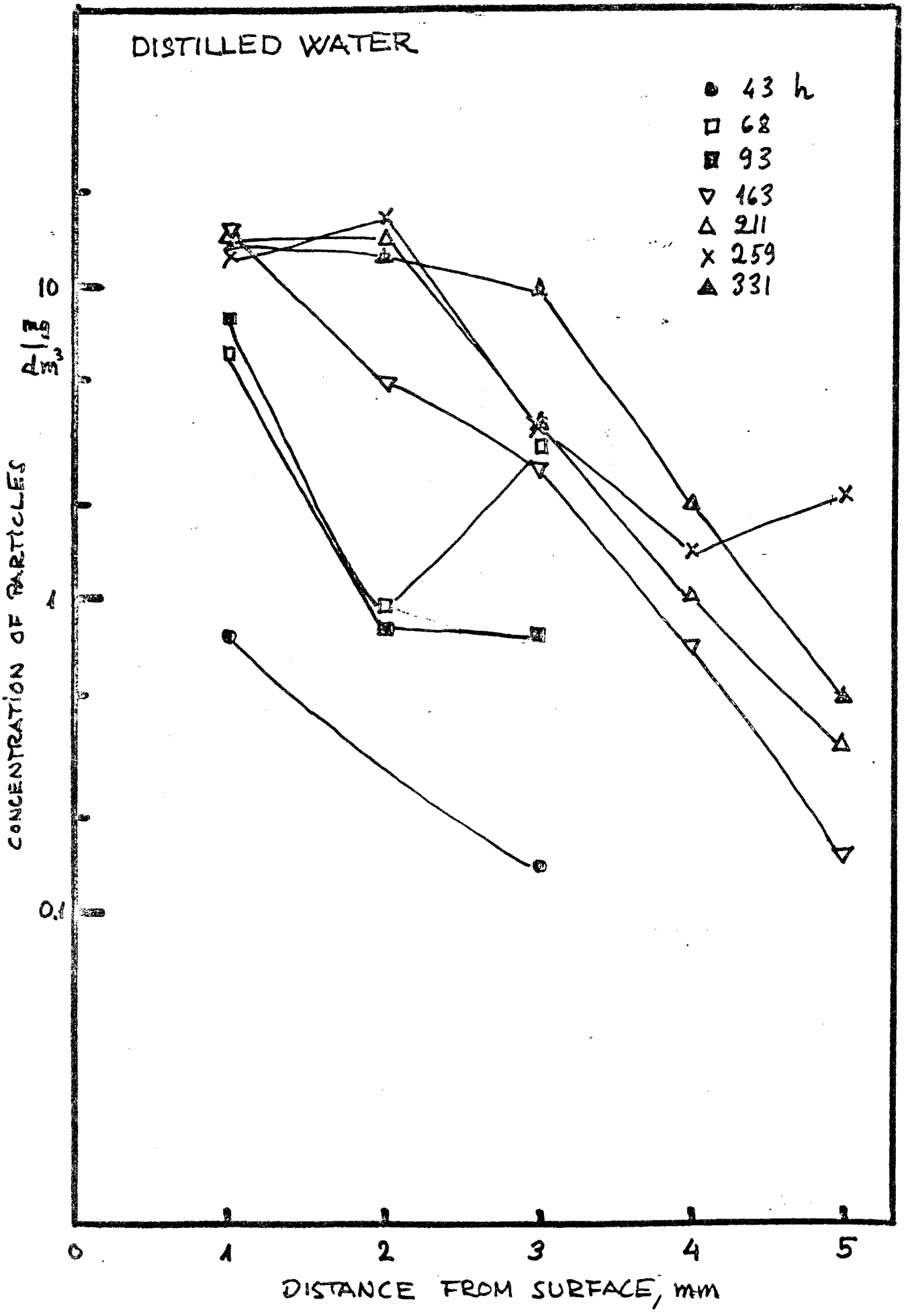
DISTILLED WATER
43 h
68
93
163
211
259
331
CONCENTRATION OF PARTICLES
10
1
0.1
0
1
2
3
4
5
DISTANCE FROM SURFACE, mm

Fig. 6.1

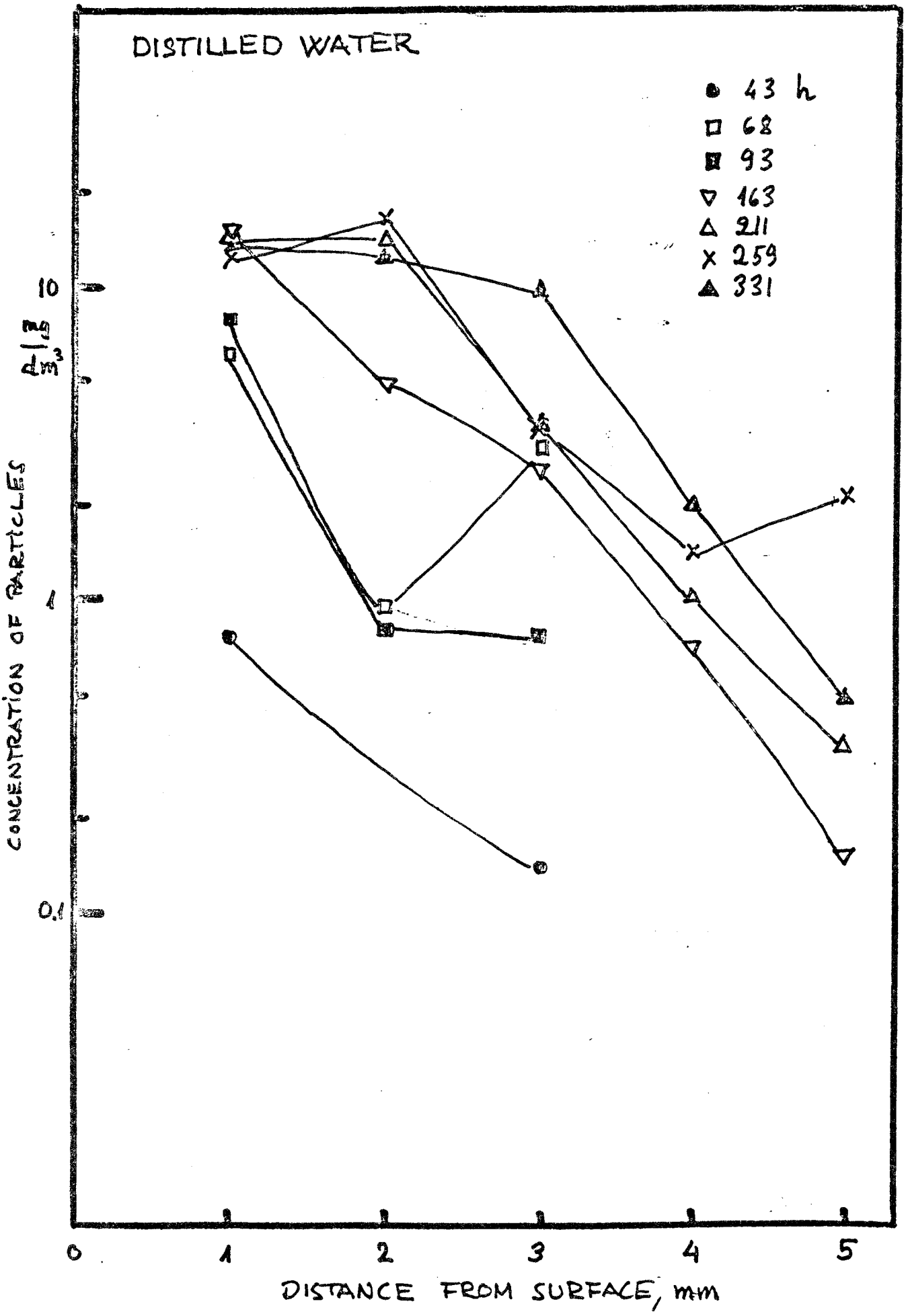
DISTILLED WATER
43 h
68
93
163
211
259
331
CONCENTRATION OF PARTICLES
10
1
0.1
0
1
2
3
4
5
DISTANCE FROM SURFACE, mm

FIG. 6.2

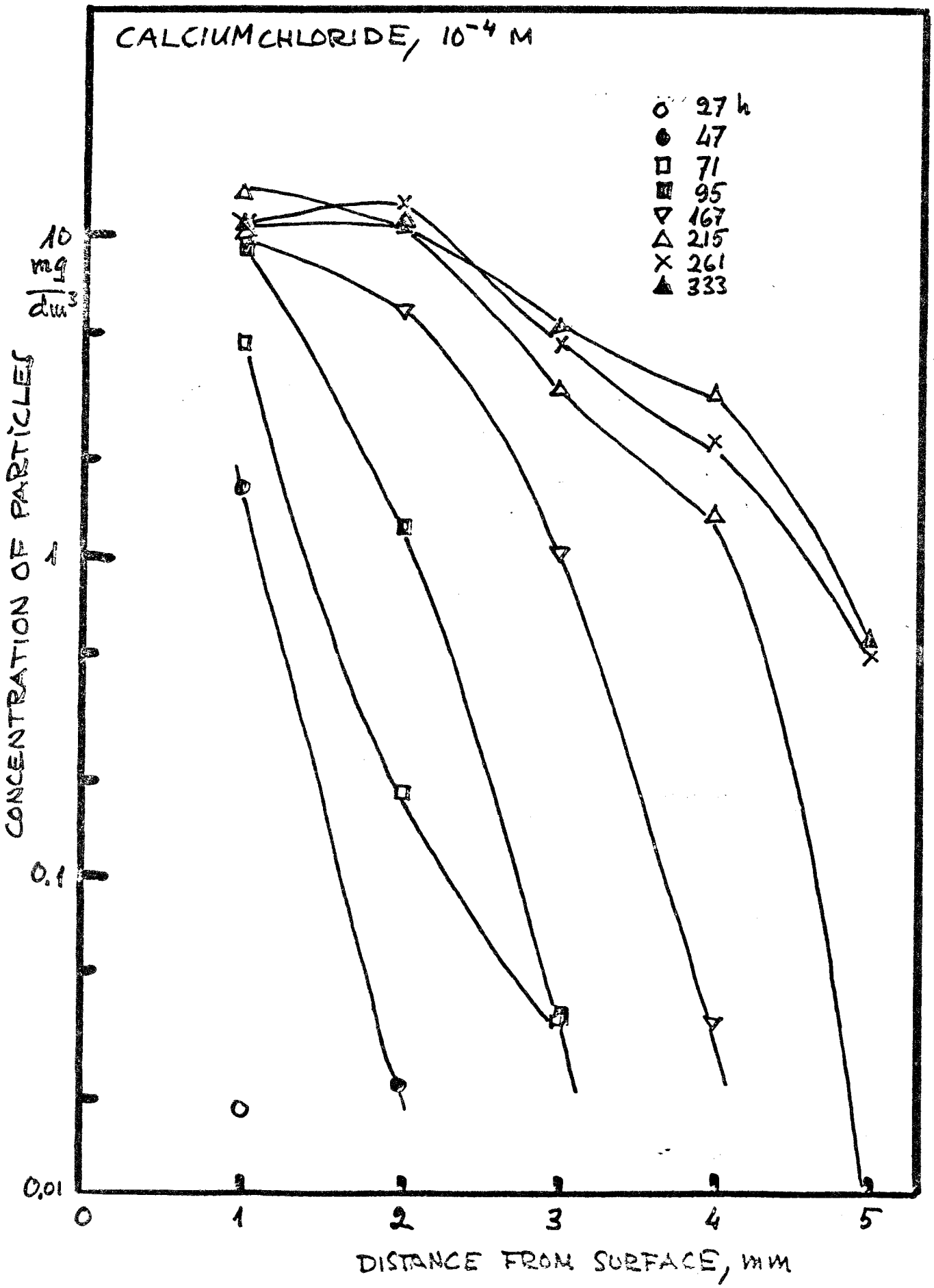
CALCIUMCHLORIDE, 10^{-4} M
27 h
47
71
95
167
215
261
333
10 mg/dm³
1
0.1
0.01
CONCENTRATION OF PARTICLES
0
1
2
3
4
5
DISTANCE FROM SURFACE, mm

FIG. 6.3

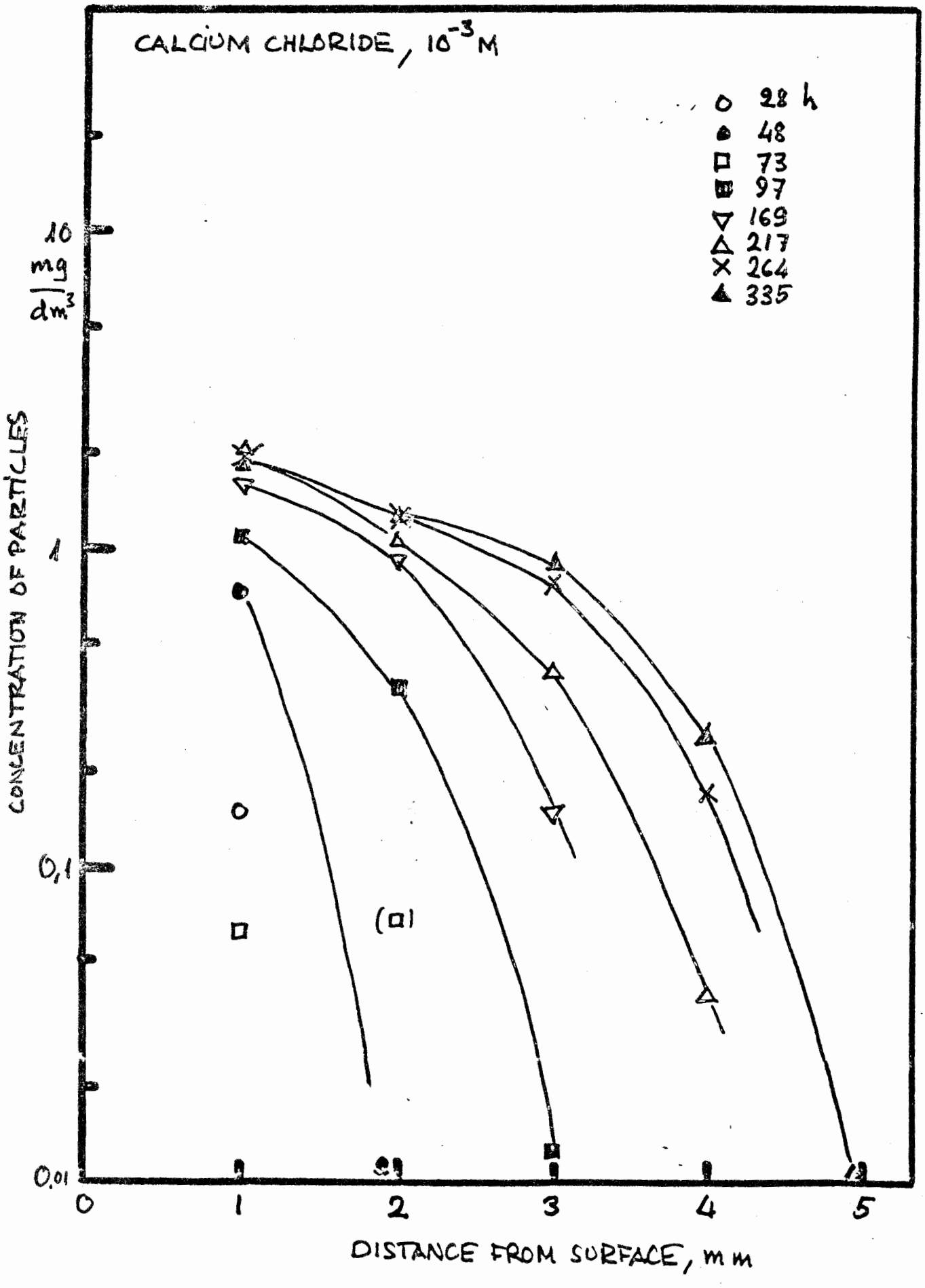
CALCIUM CHLORIDE, 10^{-3} M
28 h
48
73
97
169
217
264
335
10
1
0,1
0,01
mg/dm³
CONCENTRATION OF PARTICLES
(a)
0
1
2
3
4
5
DISTANCE FROM SURFACE, mm

FIG. 6.4

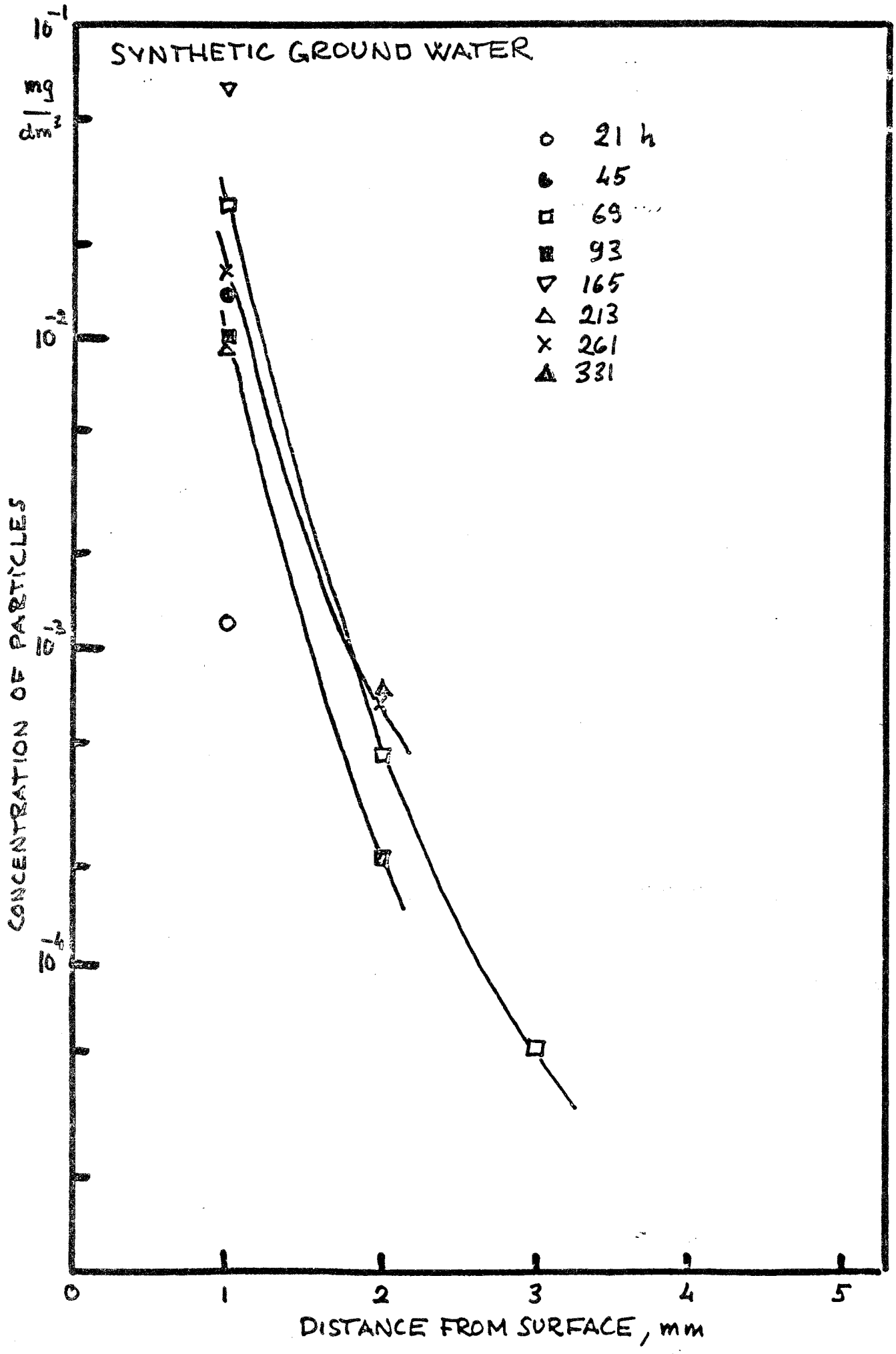
SYNTHETIC GROUND WATER
21 h
45
69
93
165
213
261
331
CONCENTRATION OF PARTICLES
mg / dm³
10⁻¹
10⁻²
10⁻³
10⁻⁴
0
1
2
3
4
5
DISTANCE FROM SURFACE, mm

difference between the release of particles from the gel in contact with synthetic ground water and the other solutions is clearly seen in fig. 6.5 which gives the particle concentration at a distance of 3 mm from the gel surface as a function of time.

4. An equilibrium concentration gradient appears to be set up after ca 250 h for the two Ca^{2+} solutions studied. The concentrations of this equilibrium is an order of magnitude smaller for 10^{-3} mol dm^{-3} Ca^{2+} than for 10^{-4} mol dm^{-3} Ca^{2+}.

The following conclusions may be drawn:

- Particles will be released from uncoagulated bentonite gel (i.e. into distilled water and 10^{-4} mol dm^{-3} $CaCl_2$)

- Particle release is an order of magnitude less for 10^{-3} mol dm^{-3} $CaCl_2$ which probably is close to the ccc of the montmorillonite (see below under 6.2).

- Synthetic ground water contains bivalent ions well above the ccc. The particle release then is so small that it is difficult to distinguish from background scattering at a distance > 1 mm from the surface. The particles that can be detected are large, which supports the fact that the gel in contact with this water is fully coagulated.

6.2 Sediment volumes

From the centrifugation experiments shown in detail in appendix 1, fig. 9-12, and summarized in figure 6.5, it can be concluded that the concentrations of divalent cations in the water will almost completely determine the properties of the bentonite gel at the water interface. It is seen that the sediment volume of bentonite in synthetic ground water lies nearly on the curve for $CaCl_2$. The deviation is

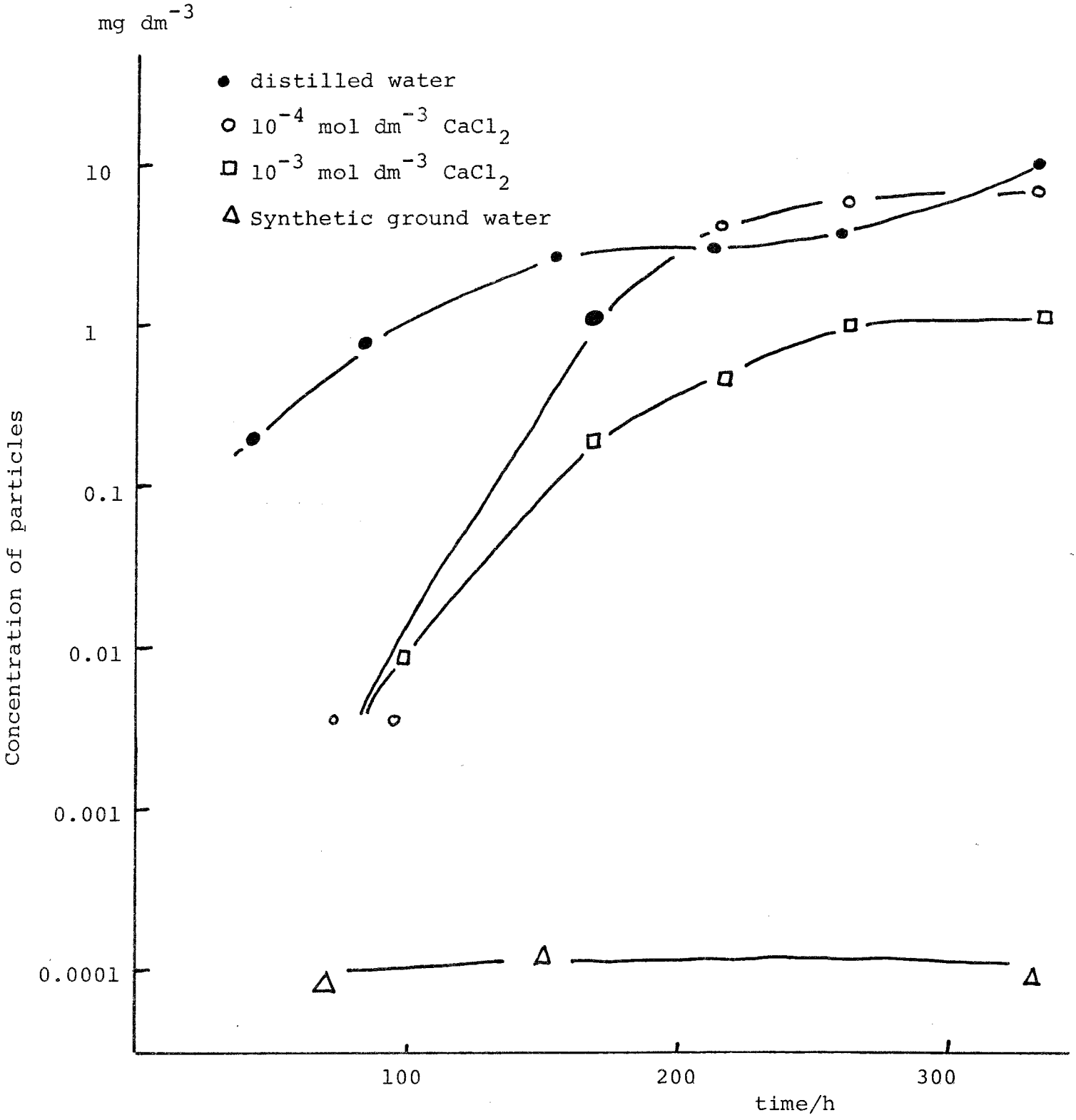

Figure 6.5. The concentration of particles 3 mm from the gel surface as a function of time.

probably due to the Na^+ content of the water which causes more efficient coagulation. These data are in accordance with other investigations found in the literature. However, the high concentration of bentonite, 2%, makes it necessary to take the cation exchange capacity into account. The following calculation can be made (45):

Total cation exchange capacity (c.e.c) of Bentonite MX-80 = 81.7 meq /100 g, of which $Ca^{++} + Mg^{++} \approx$ 55-60 mg /100 g and Na^+ 20-40 meq /100 g.

The exchangeable Na^+ is 20-35 meq /100 g, equivalent to 4.0-7.0 meq Ca^{++} or Mg^{++}/dm^3 of a 2% suspension.

Synthetic ground water contains~2 meq Ca^{++} and~0.5 meq Mg^{++}/dm^3, i.e. the total concentration of bivalent cations is 2.2/2 = 1.1 mmol/dm^3 while the Na^+ concentration is 5.4 mmol dm^{-3}.

Hence, the bivalent ion content of a suspension of 2% bentonite in synthetic ground water is not sufficient to exchange all the sodium in the gel. 5 mmol dm^{-3} $CaCl_2$ (10 meq Ca^{++}/dm^3) should, on the other hand, be able to exchange all the sodium. Fig. 6.6 shows that the volume of the sediment is further decreased from that for the synthetic ground water at this concentration, indicating complete coagulation. The decrease in sediment volume indicating face-to-face coagulation begins at concentrations far below that of the ground water.

Thus, the behaviour of the sediment volumes clearly shows that coagulation can be achieved with synthetic ground water. The high sodium content (well above the c.c.c. for Ca-montmorillonite, tab. 4.1) is enough to coagulate the clay. Electrophoretic mobility data (28) show that there is a decrease in mobility already when the exchangeable sodium is less than 30% of the c.e.c. This is probably why the sediment volumes decrease at relatively low Ca^{++} concentrations.

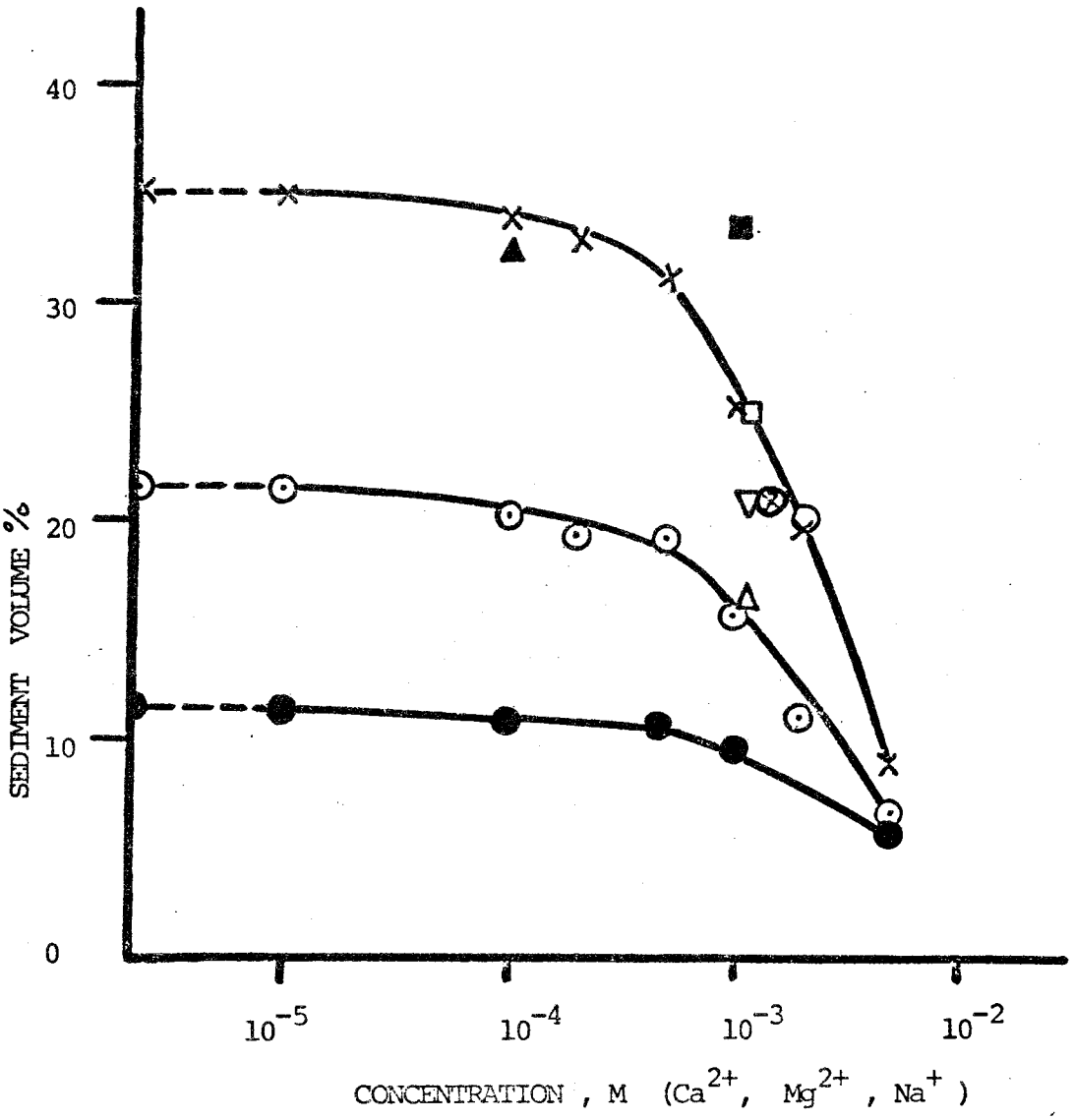

Figure 6.6 The relative sediment volume of initially 2% bentonite suspensions after centrifugation as a function of the concentration of ions in the surrounding water
Drawn curves: $CaCl_2$. Other points: (all conc. in mol dm^{-3})

▲ Mg^{++}, 10^{-4}

■ Na^{+}, 10^{-3}

○ Mg^{++}, 10^{-3} + Ca^{++}, 10^{-3}

▽ Mg^{++}, 10^{-3} + Ca^{++}, 10^{-4}

△ Mg^{++}, 10^{-4} + Ca^{++}, 10^{-3}

□ Ca^{++}, 10^{-3} + Na^{+}, 10^{-3}

⊗ Synthetic ground water: Ca^{++} ,0.83×10^{-3};Mg^{++};2.8×10

Relative centrifugal forces:

× 500x g

⊙ 3150x g

● 12600x g

for $CaCl_2$. All other points are given for 500x g.

The light scattering (l.s.) experiments show that the coagulated structure is rigid enough to make particle release negligibly small. The c.e.c. of a 15% gel (as studied with l.s.) is too high to allow exchange of the whole gel into equilibrium with ground water. Apparently, the coagulated structure formed at the gel surface is, nevertheless, sufficiently rigid to prevent particle release completely.

6.3 Sedimentation stability

The results from the studies of the sedimentation from gel tubes with their open end downwards are reported in table 6.1. At $CaCl_2$ concentrations > the c.c.c. and in synthetic ground water the gel is coagulated into a structure which prevents dispersion into the underlying water. There is no difference between experiments with circulating or non-circulating water. Again, the conclusion is that the gel surface is coagulated into a structure that prevents dispersion as soon as the surface layer has been cation exchanged.

Table 6.1

Sedimentation from gel surface (15% MX-80 bentonite in distilled water) in contact with different waters

1. No circulation of water

	Composition	Observation
a.	Distilled water	sediments (ca 60h)
b.	Synth. ground water	no change
c.	$CaCl_2$, 10^{-4}M	sediments
d.	" , 10^{-3}M	swells somewhat
e.	" , $5 \cdot 10^{-3}$M	"-

2. Circulation of water

	Composition	Observation
a.	$CaCl_2$ $2 \cdot 10^{-4}$	sediments (ca 79h)
b.	" $5 \cdot 10^{-4}$	"-
c.	" $1 \cdot 10^{-3}$	no change
d.	" $2 \cdot 10^{-3}$	"-
e.	Synth. ground water	"-

6.4 Diffusion

The diffusion of calcium ions and sodium lignosulphonate (NaLS) into 4% bentonite gel was studied.

The results of the NaLS experiment was somewhat inconclusive. Duplicate experiments were performed. In one sample no NaLS was detected in any of the gel slices from the test tubes. In the other sample, the concentration after 218 h at a depth of 5 mm was approximately equal to that of the initial solution. The diffusion coefficient calculated from the total amount of LS diffused to 15 mm beneath the surface in this sample is $1.9 \cdot 10^{-9}$ m^2 s^{-1}, which is of the same order as that of Ca^{2+}. No NaLS was found below 15 mm.

Taking the diameter of the NaLS molecule as ≈ 6 nm (viscosity measurements) the molecule should easily diffuse into a 4% gel; the distance between the plates in parallel arrangement is approximately 60 nm. In a bentonite at depositing depths diffusion would be impossible due to steric hindrance, even if the bentonite is swollen to its equilibrium water content (plate distance ≈ 2 nm, see below). Although the formation of wider channels between "card packs" of aligned particles may be envisaged, the diffusion of particles of colloidal size through gels at this high pressure appears highly improbable.

The diffusion of Ca^{++} ions is depicted in appendix 1, fig. 8 and is summarized in table 6.2. In this case, a diffusion coefficient could readily be determined. Due to the sodium ion content of the MX-80 bentonite, the method used here yields an "average" diffusion coefficient which includes the cation exchange taking place in the clays. Hence, it cannot be directly compared to the coefficients given in table 4.2. The diffusion is rather rapid and it is obvious that the bentonite becomes completely cation exchanged within a fairly short time. This is completely in accordance with the l.s. and sediment volume experiments, which shows that the clay is rapidly coagulated.

Table 6.2

Diffusion of Ca^{++} ions into a bentonite gel (MX-80) in contact with 0.1 mmol/dm^3 $CaCl_2$

	4% MX-80		7% MX-80	
$\frac{t}{h}$	$\frac{\bar{X}}{mm}$	$\frac{D \cdot 10^9}{m^2/s}$	$\frac{\bar{X}}{mm}$	$\frac{D \cdot 10^9}{m^2/s}$
1.0	0.9	0.12	0.75-0.8	0.11
2.75	1.7	0.15	1.2	0.07
19.75	10	0.70	6	0.25
28.0	16.5	1.4	8.5	0.36
43.5	19-20.5	1.2-1.4	10.25	0.34
118.0	27.0	0.85	18.5	0.35
188.5	31.7	0.75	21.8	0.35

4%: $\bar{D} = 1.03 \cdot 10^{-9}$ m^2/s (the two first values are omitted)

7%: $\bar{D} = 0.34 \cdot 10^{-9}$ m^2/s - " -

t = time

$\bar{X}$ = diffusion distance into gel

D = diffusion coefficient

6.5 Swelling pressure

The swelling of compacted MX-80 bentonite in the "artificial crack" was followed by measuring the distance that the bentonite front had advanced at regular intervals until, after about 100 h, the cell cracked. Photographs of the cell are given in Appendix 1. The photographs taken after the cracking of the cell clearly document that bentonite does swell into narrow cracks. The swelling distance as a function of time is given in fig. 6.7.

Visually, some orientation of the bentonite particles between the plates can be observed. Whether there is an orientation on a microscopic level has not been examined.

The initial swelling is very rapid but the rate then decreases to a constant value. There is no indication that the rate of swelling would be decreasing to zero. This is an interesting observation that has to be discussed in view of what is known about the equilibrium swelling pressure of bentonite (montmorillonite).

Equilibrium swelling pressures for pure montmorillonite have been measured by several authors. Some results are collected in fig. 6.8. As discussed in chapter 4.4., the swelling pressure is due to double layer repulsion and, hence, both concentration and charge of the cation is of importance. It is stressed that those curves represent equilibrium situations, i.e., at a given pressure and electrolyte composition, the gel will swell to a given plate distance and then stop swelling.

From fig. 6.8 it can be seen that when the electrolyte concentration (NaCl) is increased from 0.1 to 100 mmol/dm^3 in a 40% bentonite suspension (corresponding to a plate distance of $\approx$ 4.5 nm) the swelling pressure drops from 10 atm to about 3 atm; if divalent cation is substituted for Na^+ the swelling pressure drops to 0.1-0.3 atm. For ground water the swelling pressures consequently will be quite low.

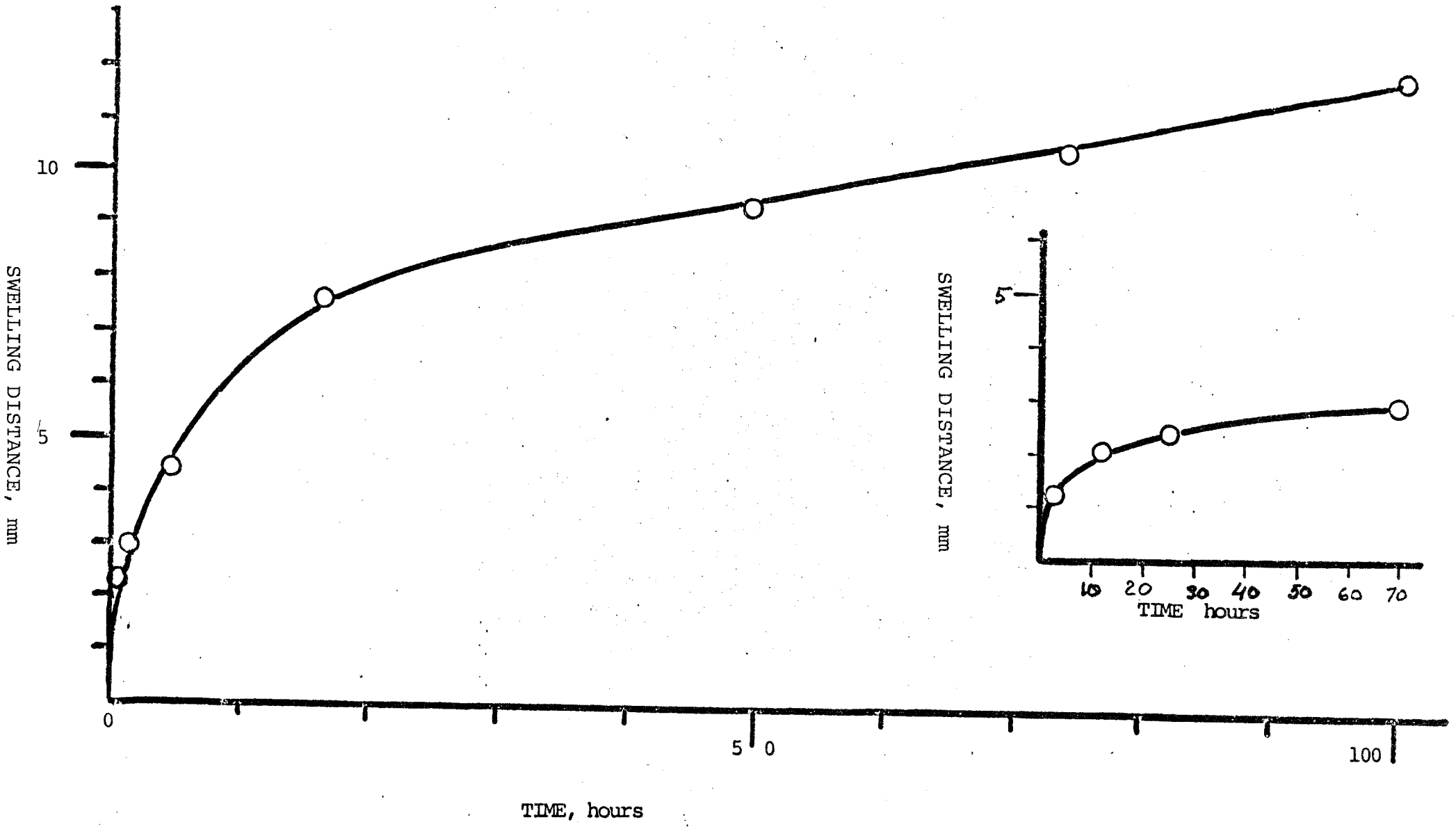

Fig. 6.7. The swelling of compacted bentonite into an artificial crack of thickness 0.5 mm, filled with artificial ground water.

FIG. 6:8

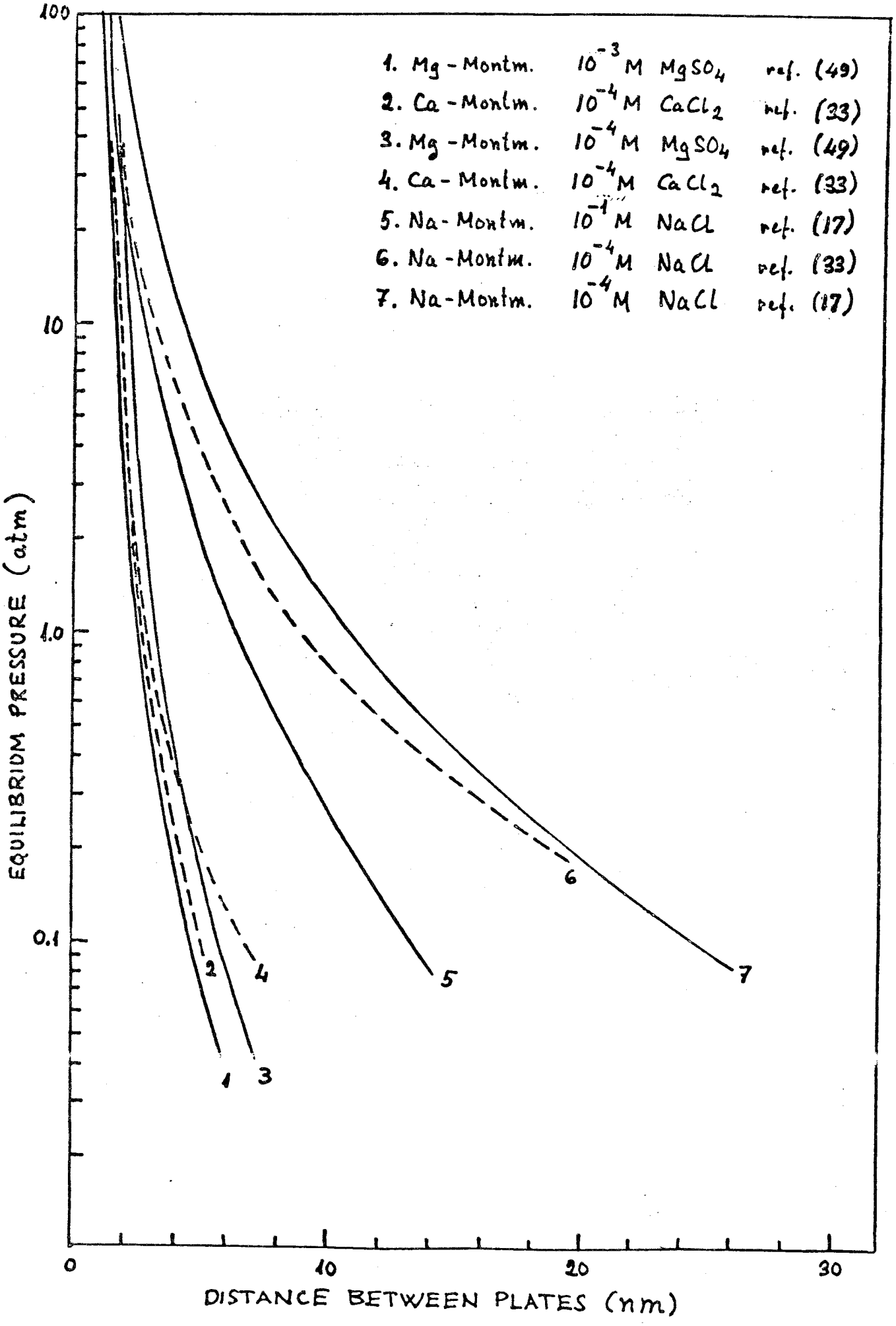
1. Mg - Montm. 10^{-3} M $MgSO_4$ ref. (49)
2. Ca - Montm. 10^{-4} M $CaCl_2$ ref. (33)
3. Mg - Montm. 10^{-4} M $MgSO_4$ ref. (49)
4. Ca - Montm. 10^{-4} M $CaCl_2$ ref. (33)
5. Na - Montm. 10^{-1} M NaCl ref. (17)
6. Na - Montm. 10^{-4} M NaCl ref. (33)
7. Na - Montm. 10^{-4} M NaCl ref. (17)
100
10
1.0
0.1
EQUILIBRIUM PRESSURE (atm)
0
10
20
30
DISTANCE BETWEEN PLATES (nm)

The water content of the compacted bentonite will be about 15%, corresponding to a calculated plate distance of < 0.45 nm. At the suggested depths of waste disposal the hydrostatic pressures are in the range 50-100 atm, which will not affect the swelling pressure markedly. The equilibrium plate distance will, thus, be about 1.5-2.0 nm (fig. 6.8 ref. 17). Thus, the equilibrium water content will be approximately three to four times that of the compacted bentonite. Taking the bentonite particle thickness as 1 nm, the increase in volume when the compacted bentonite swells until equilibrium is attained will be about 60-100%. Hence, if allowed to swell freely, a bentonite deposit of the suggested shape, a cylinder of thickness $\sim$ 0.4 m and outer radius 150 cm, will swell from a radius of 150 to 170 cm or be able to fill 10 concirculating cracks of widths 1 mm to a length of 13-16 m.

However, it should be noted that this calculation assumes that the bentonite is in equilibrium with water at 1 atm. As is argued in appendix 3, if the surrounding water is at the same pressure as the clay, it will swell until the swelling pressure is equal to the pressure in the bulk liquid, i.e. the distance corresponding to 1 atm in fig. 6.8 is valid for equilibrium with water at 1 atm. The equilibrium distance then is 2 nm corresponding to a dilution of the clay to about 65-70% water.

In our opinion, the results of the swelling experiment in the "artificial crack" clearly indicates that the gel will continue swelling at a steady rate even in a narrow crack. If the total available crack volume is large enough there might be a gradual dilution of the clay to about 70% water content at the pressures obtained at the suggested depositing depth.

The possibility that the flow of bentonite into the cracks might be prevented by the flow properties of the clay should be considered. Bentonite suspensions are considered to behave like Bingham bodies. The flow thus depends on the magnitude of the yield stress exhibited by bentonite suspensions of these concentrations under very low shear rates. If the suspension exhibits ideal Bingham characteristics, plug flow

would occur. The bentonite then would flow out as long as a pressure gradient exists. The swelling experiment in the "artificial crack", although admittedly conducted under a short period of time (100 h) is completely in accordance with this conclusion.

In the cracks there will be set up a particle concentration gradient which opposes the flow. The divalent cations of the ground water will gradually exchange the cations in the clay, thus lowering the ccc of the initial Na-Cl-montmotillonite and ensuring coagulation of the clay. This coagulation will probably decrease the rate of flow into the cracks.

7. Conclusions and suggestions

From literature data and the experiments reported here the following picture of the behaviour of the bentonite gel emerges:

1. Although MX-80 is a mixed sodium-calcium bentonite it will be completely ion exchanged into a calcium bentonite when brought into contact with ground water.

2. This ion exchange in combination with the composition of the ground water ensures that the clay will be completely coagulated by the ground water.

3. The coagulated structure does not release detectable amounts of particles from the clay surface into ground water, whether the surface is subjected to realistic circulation of water or gravitational forces.

4. The gel does release particles into distilled water and dilute electrolyte solutions. The concentration of these, however, is an order of magnitude less than the most pessimistic predictions for ground water. Hence, there appears to be negligible change that particles will be released from the gel. However, due to the extreme polydispersity of montmotillonite tiny particles of a few nanometres in size might not be easily detectable by light scattering.

5. The equilibrium composition of a (coagulated) bentonite gel at 50 atm in contact with ground water at 1 atm is a water content of 65-70%. The equilibrium composition of gel at 50 atm in contact with ground water at the same pressure is also a water content of 65-70%. Since the water content of the compacted bentonite is about 15%, it will spontaneously swell to a volume that is 60-100% larger than the original volume. This ensures that the cracks surrounding the bentonite will be filled by swelling as has been experimentally demonstrated.

6. There is, in our opinion, nothing that suggests that the gel would not swell to this equilibrium volume if it is available. Although particles will not leave the gel even after such a swelling has taken place, the permeability of the bentonite mass certainly would be substantially increased (thickness of water layers between the plates 1.5 -2.0 nm).

Hence, one should consider whether it is possible that the crack volume available to the bentonite mass could be larger than 60-100% of the original volume of the mass. In that case, the probability of obtaining a more permeable bentonite mass should not be overlooked. One way of overcoming this problem is to maintain a pressure difference between water and clay corresponding to the equilibrium plate distance obtaining in 85% bentonite.

The only way to ensure whether viscosity and yield stress values of the gel would actually prevent swelling to equilibrium, in our opinion, is to measure these quantities under realistic pressures for concentrated bentonite suspensions at very low shear rates.

REFERENCES

1. Verwey, E J W, Overbeek, J Th G
   Theory of the stability of Lyophobic Colloids
   Esevier, Amsterdam, 1948.

2. Derjaguin, B V, Landau, L
   Acta Physicochim URSS, 14, 633 (1941).

3. Ottewill, R H et al in
   Colloid Science (Specialist Periodical Report)
   Vol. 1 and 2, The Chemical Soc., London 1973 and 1975

4. Sonntag, H and Strenge, K
   Coagulation and Stability of Disperse Systems
   Halstead Press, 1970.

5. Kruyt, H R
   Colloid Science, vol 1 Elsevier, New York 1952.

6. van Olphen, H
   An introduction to Clay Colloid Chemistry
   Interscience, New York, 1963.

7. Grim, R E
   Clay Mineralogy
   2nd Ed. McGraw-Hill, New York, N.Y., 1968.

8. Goodwin, J W
   Trans.Brit. Ceram. Soc. 70, 65 (1971).

9. Flegmann, A W, Goodwin, J W and Ottewill, R H
   Proc. Brit. Ceram. Soc. 31,1 (1969).

10. Schofield, R K and Samson, H R
    Disc. Faraday Soc. 18, 135 (1954).

11. van Olphen, H
J Colloid Sci, 19, 313 (1964).

12. Forslind, E and Jacobsson A
Water, a comprehensive treatise
Ed. F Franks, vol 5, Plenum Press, New York, 1975.

13. Rand, B and Melton, I E
J Colloid Interf. Sci. 60, 308, 321 1977

14. Hunter, R J and Alexander A E
J Colloid Sci. 18, 833 (1963).

15. Nicol, S K and Hunter R J
Aust. J. Chem. 23, 2177 (1970).

16. Michaels, A S and Bolger, J C
Ind. Eng. Chem. Fundam. 1, 153 (1962).

17. Barclay, L M and Ottewill, R H
Spec. Faraday Disc. 1, (1970) 138

18. Weiss, A, Hübich A and Weiss A
Ber. Deut. Keram. Ges. 41, 687 (1964).

19. Bolt, G H
Soil Sci. 79, 267 (1955)

20. Shainberg, I and Kaisermann A
Soil Sci. 104, 410 (1967).

21. Lee Swartzen-Allen and Matijevic
J Colloid Interf. Sci. 50, 143 (1975).

22. Ibid,
56, 159 (1976).

23. Norrish, K
Disc. Faraday Soc. 18, 134 (1954).

24. Posner, A M and Quirk, J P
Proc. Roy. Soc. Ser. A 278, 35 (1964).

25. Warkentin, B P and Schoefield, R K
Clays Clay Miner 7, 343 (1960).

26. Warkentin B P and Schoefiled, R K
J. Soil Sci. 13, 98 (1962).

27. Lagaly, G, Stange, H and Weiss, A
Kolloid Z Z Polym., 250, 675 (1972).

28. Bar-On, P, Shainberg, I and Michaeli, I
J Colloid Interface Sci., 33, 471 (1970).

29. Kahn, A
J Colloid Sci., 13, 51 (1958).

30. Williams, B G and Drover, D P
Soil Sci., 104, 326 (1967).

31. van Olphen, H
Clays and Clay Min. Natl. Res. Council Natl.
Acad. Sci. (U.S.) Publ. no 327, Washington, D.C., 1954.

32. Bolt, G H and Miller, R D
Soil Sci. Soc. Amer. Proc., 19, 285 (1955).

33. Warkentin, B P, Bolt, G H and Miller, R D
Soil Sci. Soc. Amer. Proc. 21, 495 (1957).

34. Barclay, L, Harrington, A and Ottewill, R H
Kolloid Z Z Polym., 250, 655 (1972).

35. Callaghan, I C and Ottewill, R H
Disc. Faraday Soc., 57, 110 (1974).

36. Hemwall, J B and Low, P F
Soil Sci. 82, 135 (1956).

37. van Olphen, H
J Colloid Sci., 20, 822 (1965).

38. Lai, T M and Mortland, M M
Clays and Clay Minerals, 9, 229, (1962).

39. Clavet, R
Ann. Argon. 24, 135 (1973).

40. Dufey, J E and Landelout, H G
J Colloid Interface Sci. 52, 340 (1975).

41. Dufey, J E and Landelout, H G
J Colloid Interface Sci., 51, 278 (1975).

42. Turk, J
Dissertation, University of California, San Diego (1976).

43. "Physical characteristics of Volclay bentonite"

44. Rennerfelt, J
KBS-report "Composition of ground water in deep layers of bedrock, 1977-11-07.

45. Jacobsson, A
Div. Soil. Mech, Univ. of Luleå,
personal communication.

46. Rennerfelt, J
Communication 21.11, 1978-01-26.

47. Stenlund, B
Dissertation, Åbo Academy, Finland (1970).

48. Gupta, P R and McCarthy, I L
Macromolec. 1, 236 (1968).

49. Ottewill, R H
Personal Communication

50. Jost, W
Diffusion in solids,liquids,gases.
Academic Press Inc., New York, 1952.

Appendix 1

ORRJE & CO
SCANDIACONSULT
Stockholm

J Rennerfelt/IP

SYNTETISKT GRUNDVATTEN (oxiderande miljö)

1978-01-24

52.2684-01

	mg/l	HCO_3^-	Ca^{2+}	Mg^{2+}	Na^+	K^+	Fe^{2+}	Mn^{2+}	SiO_2	NH_4	NO_3^-	Cl^-	F^-	NO_2^-	SO_4^{2-}	Fe^{3+}	OH^-
$NaHCO_3$	261	189,5			71,5												
$KHCO_3$	12,8	7,8				5											
$MnSO_4$	1,36							0,5							0,86		
$(H_4N)_2SO_4$	0,73									0,2					0,53		
NaF	2,21				1,21								1				
$NaNO_3$	1,37				0,37						1						
$NaNO_2$	0,15				0,05									0,1			
$Na_2SiO_3 \cdot 9\ H_2O$	94,7				15,3				20								
$CaCl_2$	7,0		2,5									4,5					
$MgCl_2$	39,2			10								29,2					
Na_2SO_4	25,4				8,2										17,2		
NaCl	8,7				3,4							5,3					
$Ca(OH)_2$	69,3		37,5														(31,8)
$Fe(III)Cl_3 \cdot 6\ H_2O$	2,4											1,0				0,5	
Summa	mg/l	197,3[x]	33	7	124	5	0	0,5	20	0,2	1	30	1	0,1	18,6	0,4	

x = Bikarbonathalten höjs till över 300 mg/l genom bubbling med kolsyra

Analyser på naturliga vatten från Norra Uppland samt sannolika analysvärden på grundvatten

Analys	Sort	Vattenhygien art. (Wenner et al.) Forsmarksomr.	Norrskedika gruva 78 m	Hallstavik 70 m 1963	Hallstavik 175 m 1977	Forsmark I 450 m 77-09-26 x)	Forsmark I 450 m 77-10-05	Ytvatten Forsmark		Grundvatten urberg sannolik analys intervall	Grundvatten urberg sannolik analys max xx)	Saltpåverkad brunn i Uppsala-området, 100 m	Lakvatten bentonit-sand 95°C 8 dygn
Ledningsförmåga	µS/cm		580	504		440	460	121	154	400-600	1100	1920	
pH		7,1 - 7,5	7,1			8,1	7,2	7,0	6,9	7,2 - 8,5	9,0 min 6,5	8,0	
Färg	Pt mg/l		50	10				95	85				
$KMnO_4$-förbr	mg/l	16-32	32	11		32	33	73	68	5-35	50	-	140
COD_{Mn}	O_2 mg/l		8							1,2-9	12,5	-	35
Ca^{2+}	mg/l		97 som Ca	35 som Ca				9	16	20-60	100	-	
Mg^{2+}	"							16	19	15-30	150	-	
Na^+	"									(~20-40)	200	-	
K^+	"												
Fe-tot	"	0,4 - 0,7	7,9	0,12	2,0	29	15	0,26	0,22	1-20	30	0,13	
Fe^{2+}	"				0,5	11	15			0,5 - 15	30		
Mn^{2+}	"	0,1 - 0,4	1,1	0,08		0,30	0,37	0,05	0,06	0,1 - 0,5	3	0,05	
HCO_3^-	"	>90	381	246		390	390	53	55	150-400	500	92	
CO_2	"	0-14	(9 aggr)	(1 aggr)		27	21	7 (aggr)	10 (aggr)	0-25	50	0	
Cl^-	"	30-60	18	27		40	45	9	11	20-100	400	558	
SO_4^{2-}	"		<1	22		10	9	8,8	7,4	20-40	100	40	
NO_3^-	"		0,38	2		0,24	0,23	0,72	0,78	0,1 - 2	10	0,01	
PO_4^{3-}	"		0,11	0,1				<0,01	0,13	0,1 - 0,6	1	0,19	
F^-	"					1,0	1,0	-	-	0,5 - 3	8	-	
SiO_2	"		19			20	22	2,8?	17	15-40	60	14	
HS^- (tot)					<0,1	5	5	-	-	<0,2 - 5	10	-	
NH_4	mg/l		0,02	<0,1		0,04	0,14	0,10	0,04	0,1 - 0,4	5	0,02	
NO_2	"		<0,001	0,01		0,075	0,11	0,00	0,0	0,01 - 0,1	0,5	0,00	
°dH	°dH	7-14	13,6	4,9		7,3	7,3	5,0	6,6	6-15	50	12,8	
O_2	mg/l				(<0,6)	<0,01	<0,01			<0,01	1		
TU	-												
Ålder	år												

x) Grundvattnet kan vara påverkat av ytvatten.

xx) Uppskattad sannolikhet för att max.värdet ej skall överskridas är 95 %.

Table 2.

Fig 1

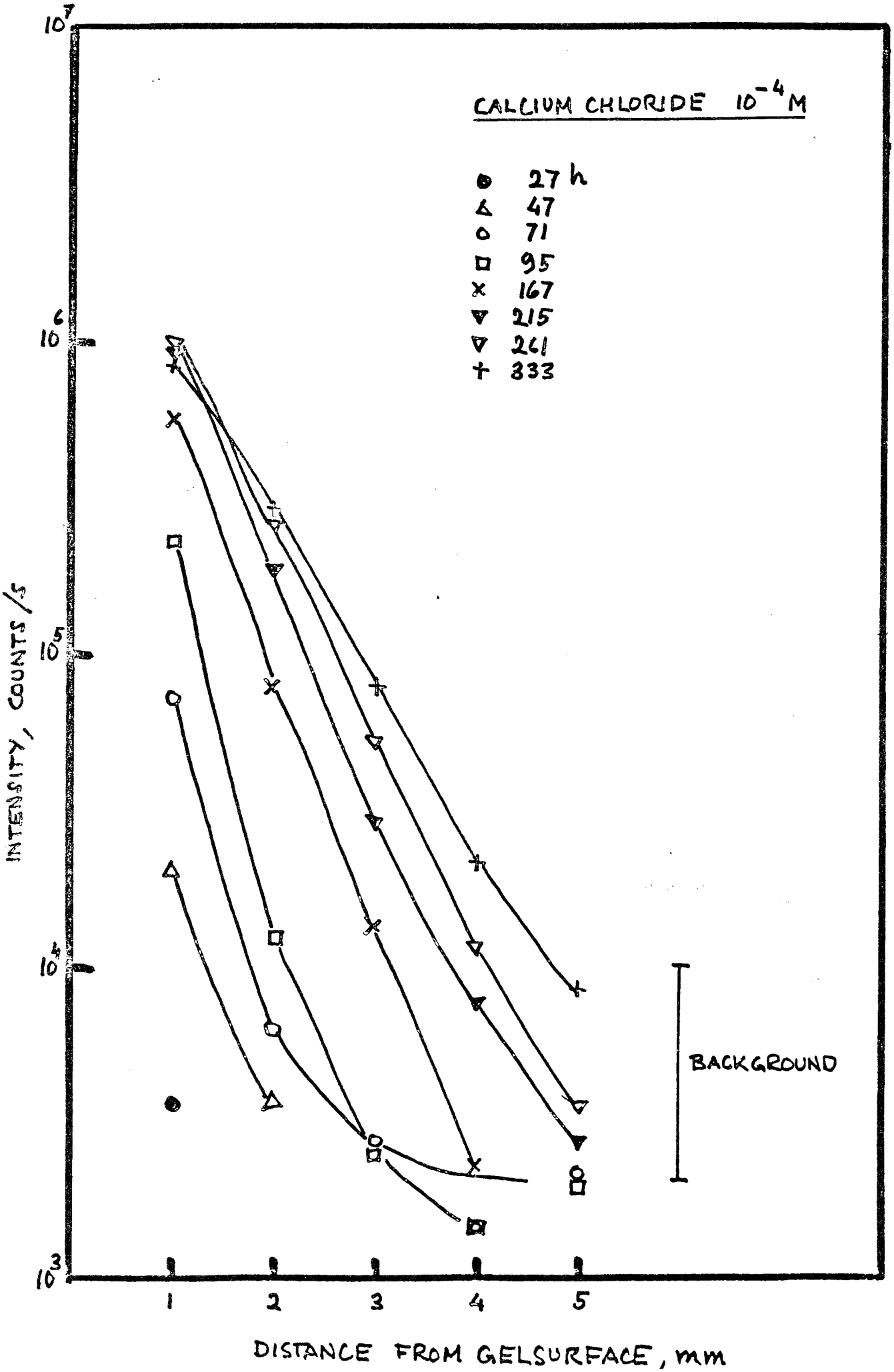
CALCIUM CHLORIDE 10^{-4} M
27 h
47
71
95
167
215
241
333
10^7
10^6
10^5
10^4
10^3
INTENSITY, COUNTS/s
BACKGROUND
1
2
3
4
5
DISTANCE FROM GELSURFACE, mm

Fig 2

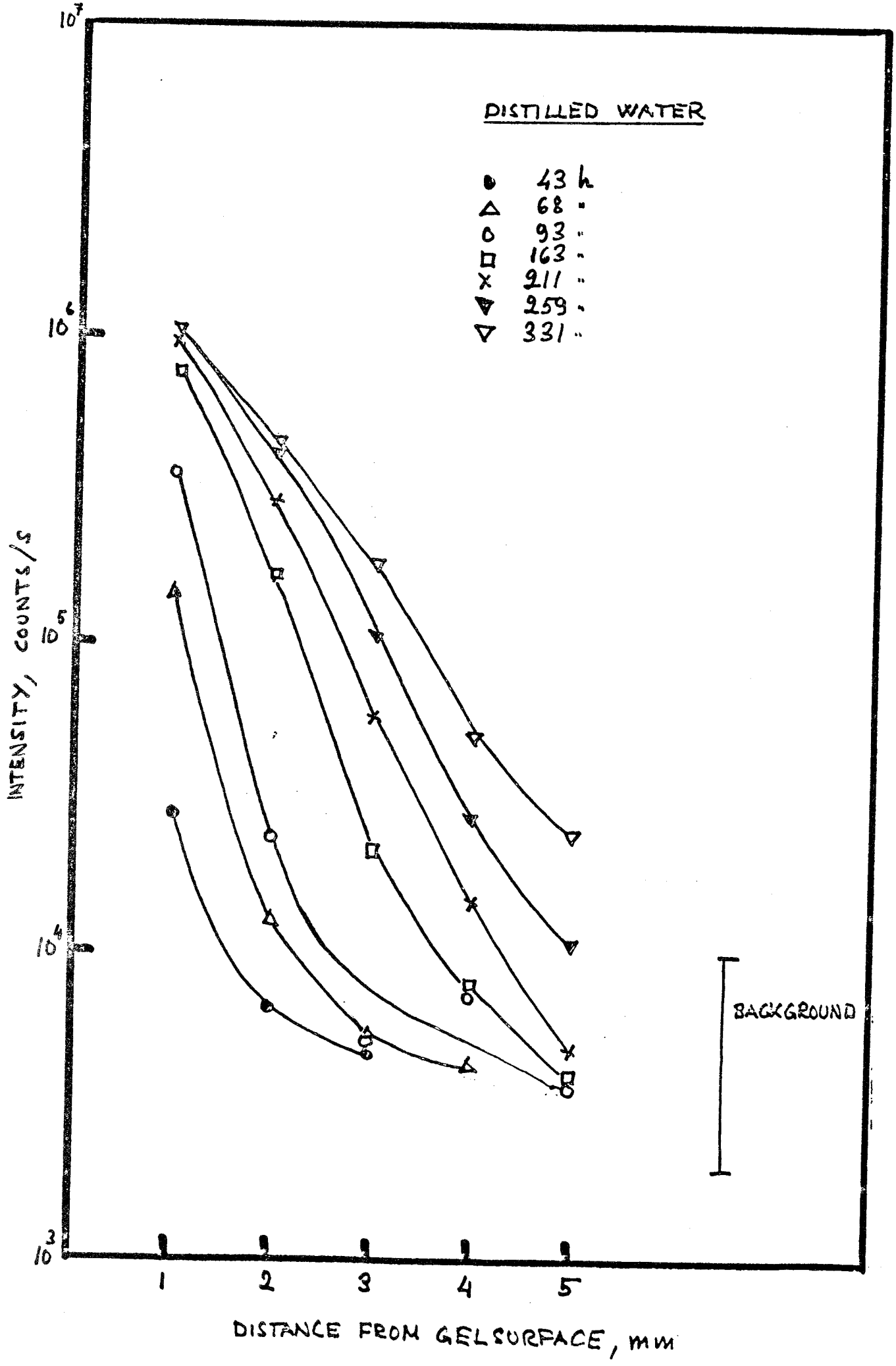
DISTILLED WATER
43 h
68 "
93 "
163 "
211 "
259 "
331 "
10^7
10^6
10^5
10^4
10^3
INTENSITY, COUNTS/S
BACKGROUND
1
2
3
4
5
DISTANCE FROM GELSURFACE, mm

Fig 3

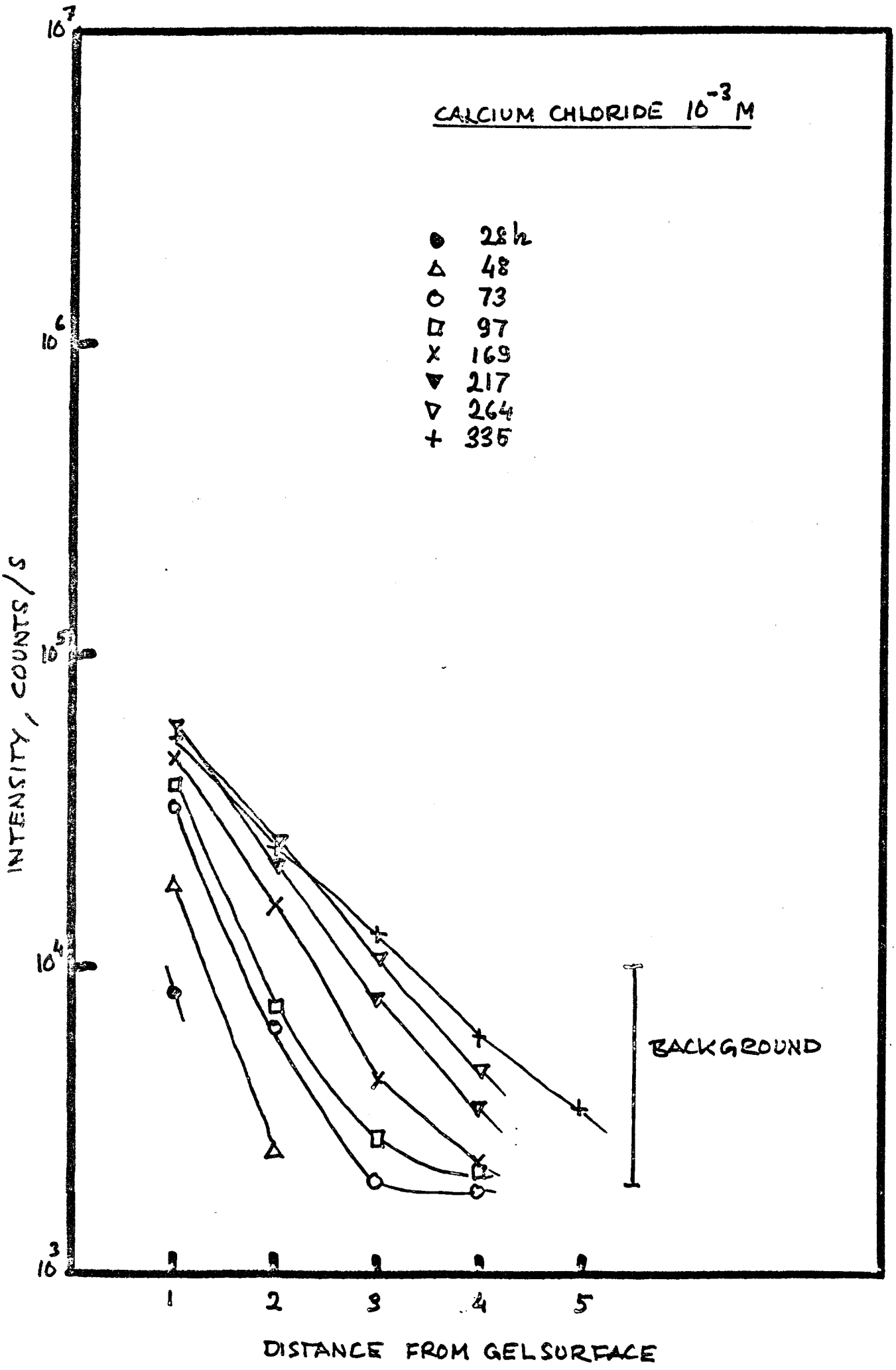
CALCIUM CHLORIDE 10^{-3} M
28 h
48
73
97
169
217
264
336
10^7
10^6
10^5
10^4
10^3
INTENSITY, COUNTS/S
BACKGROUND
1
2
3
4
5
DISTANCE FROM GEL SURFACE

Fig 4

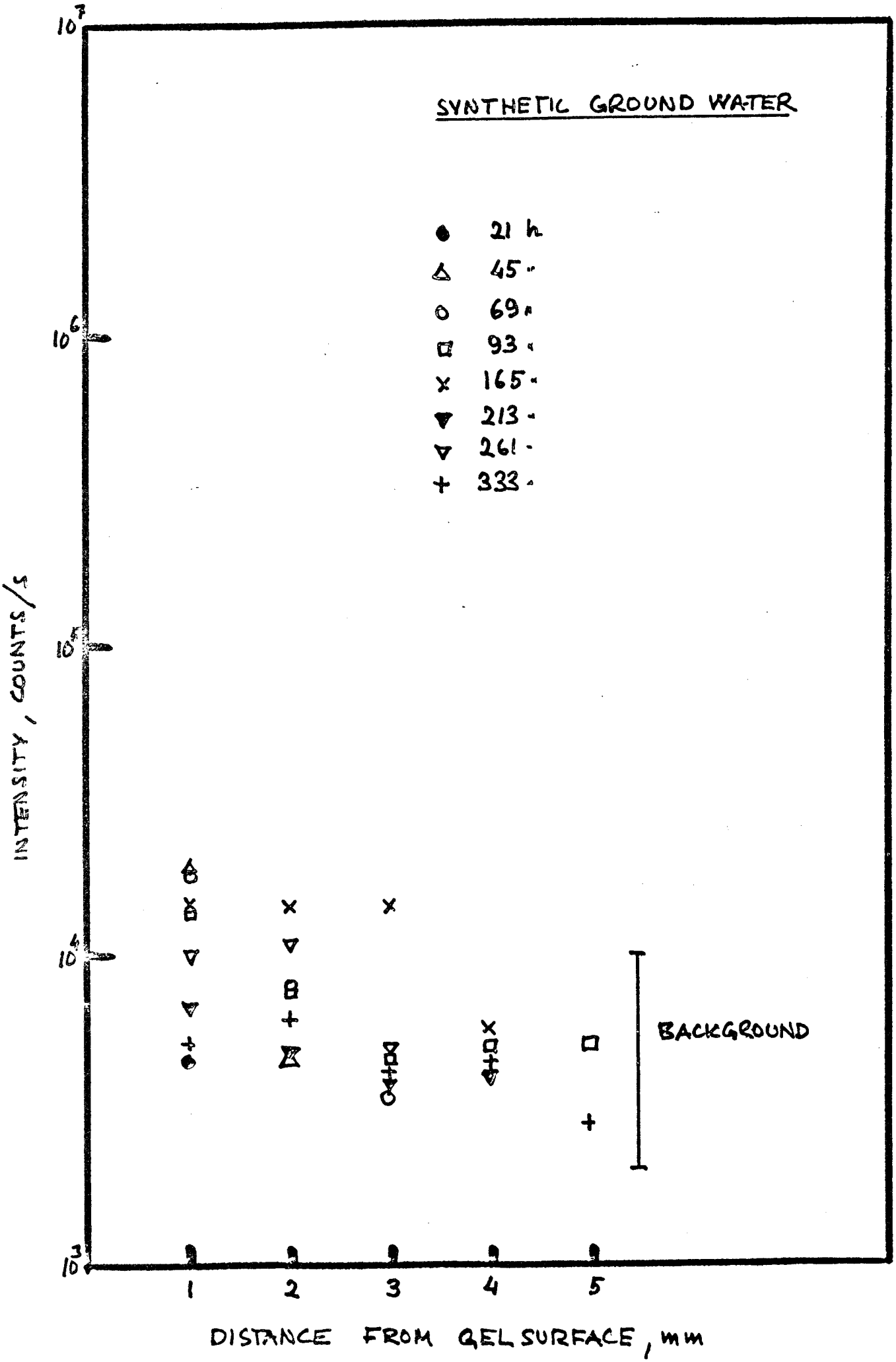
SYNTHETIC GROUND WATER
21 h
45 "
69 "
93 "
165 "
213 "
261 "
333 "
10^7
10^6
10^5
10^4
10^3
INTENSITY, COUNTS/s
BACKGROUND
1
2
3
4
5
DISTANCE FROM GEL SURFACE, mm

Fig 5

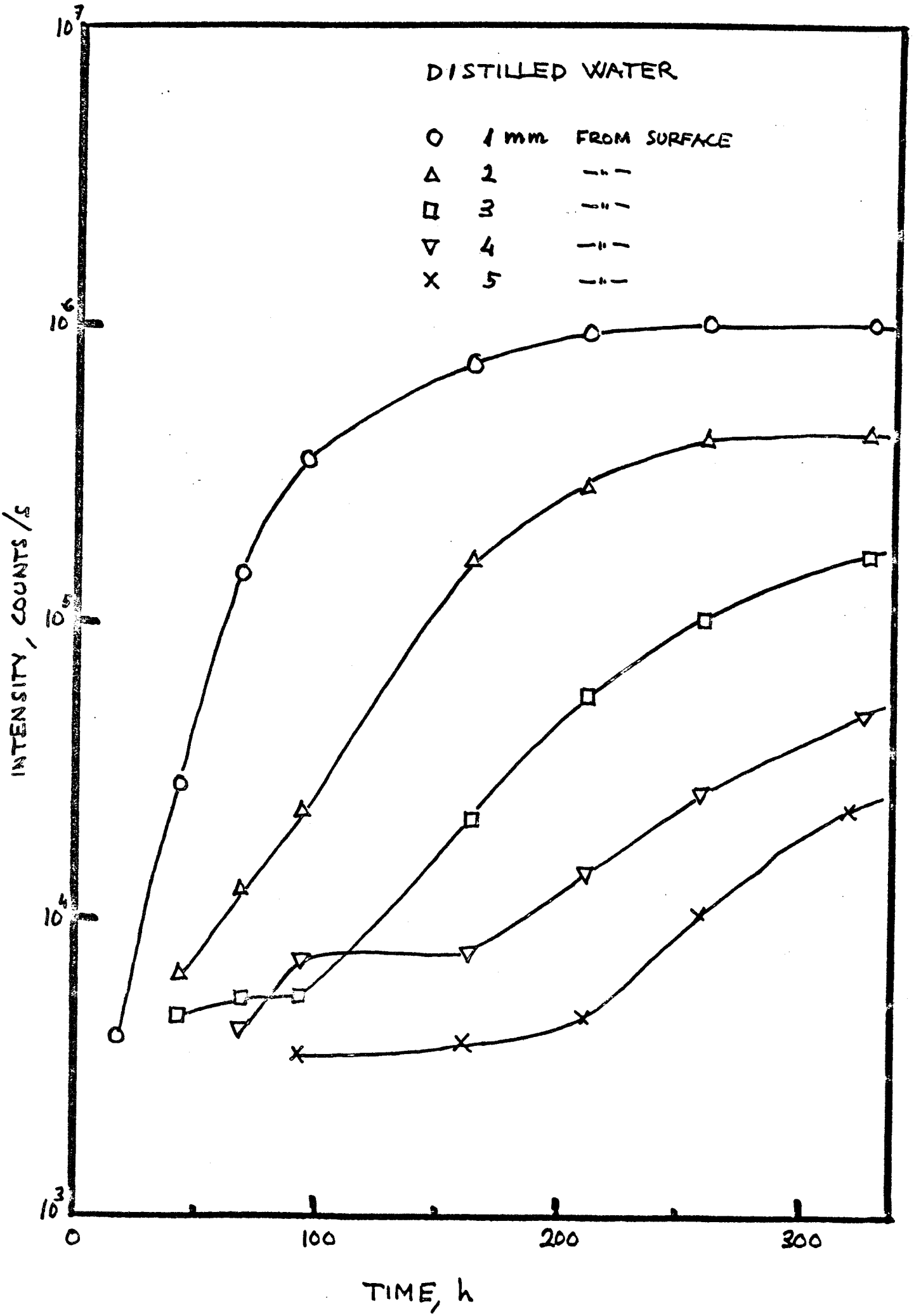
DISTILLED WATER
○ 1 mm FROM SURFACE
△ 2 —"—
□ 3 —"—
▽ 4 —"—
× 5 —"—
10^7
10^6
10^5
10^4
10^3
INTENSITY, COUNTS/s
0
100
200
300
TIME, h

Fig 6

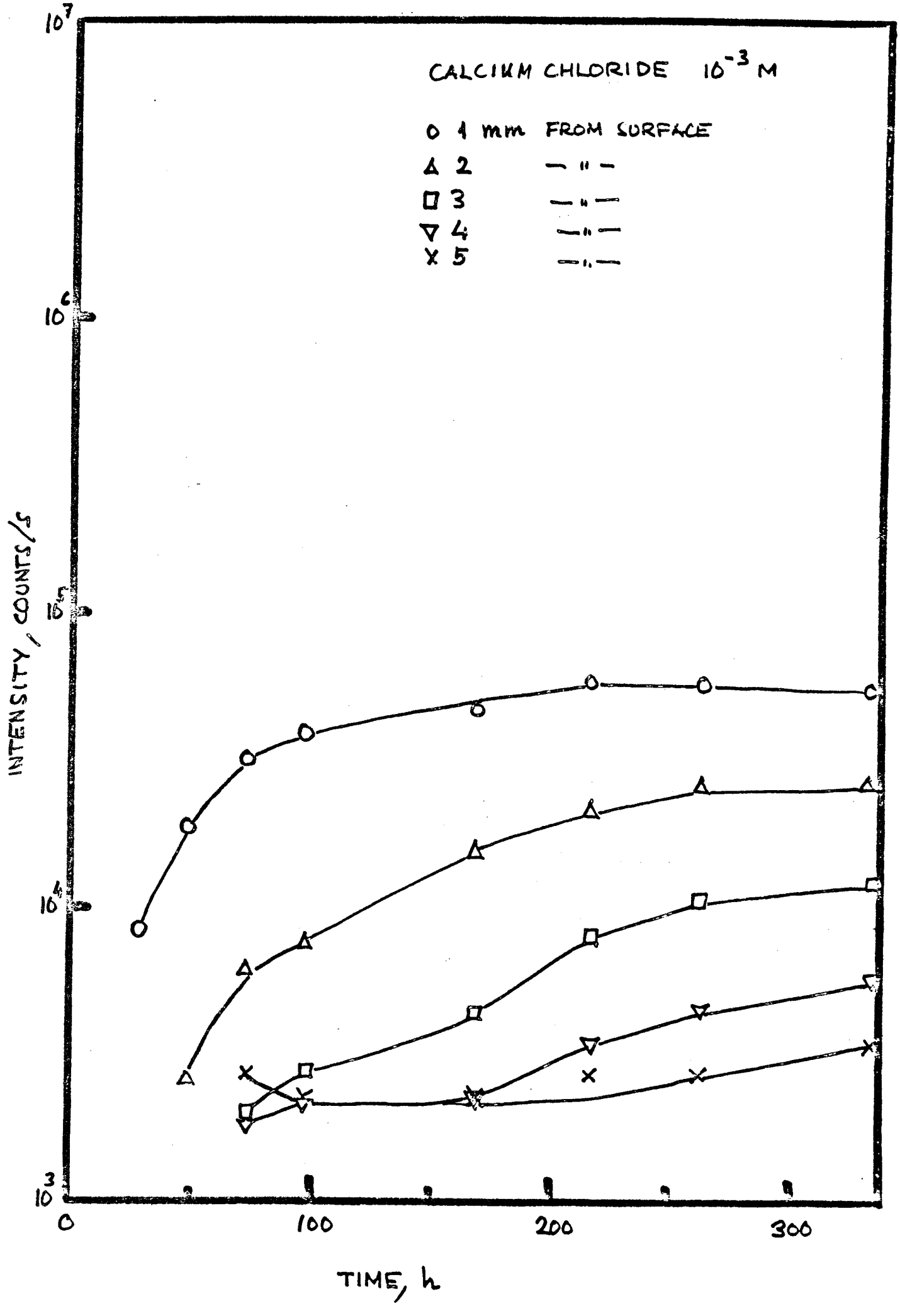
CALCIUM CHLORIDE 10^{-3} M
o 1 mm FROM SURFACE
Δ 2 — " —
□ 3 — " —
▽ 4 — " —
× 5 — " —
10^7
10^6
10^5
10^4
10^3
INTENSITY, COUNTS/S
0
100
200
300
TIME, h

Fig 7

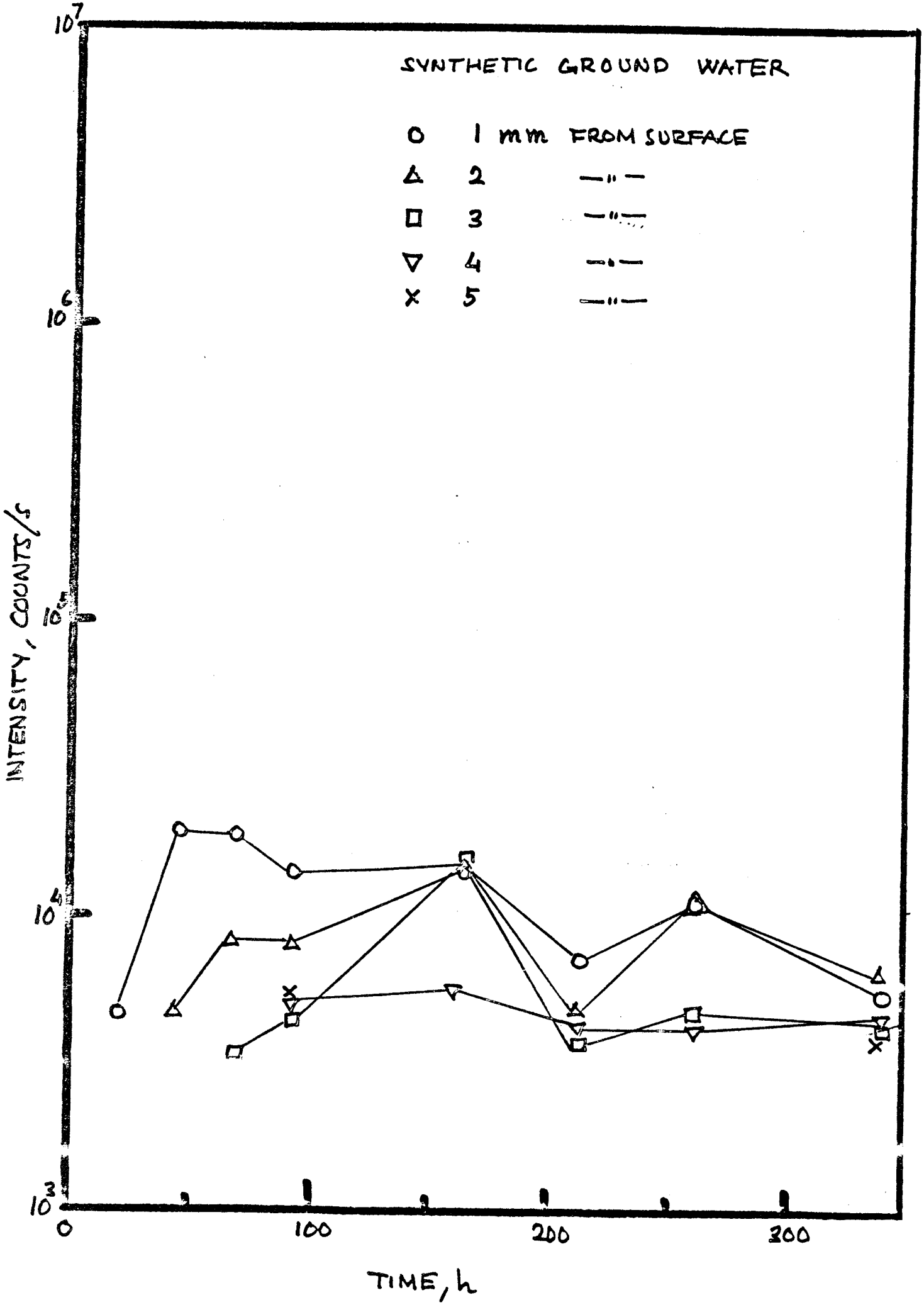
SYNTHETIC GROUND WATER
○ 1 mm FROM SURFACE
△ 2 —"—
□ 3 —"—
▽ 4 —"—
× 5 —"—
INTENSITY, COUNTS/s
10^7
10^6
10^5
10^4
10^3
0
100
200
300
TIME, h

Fig 8.

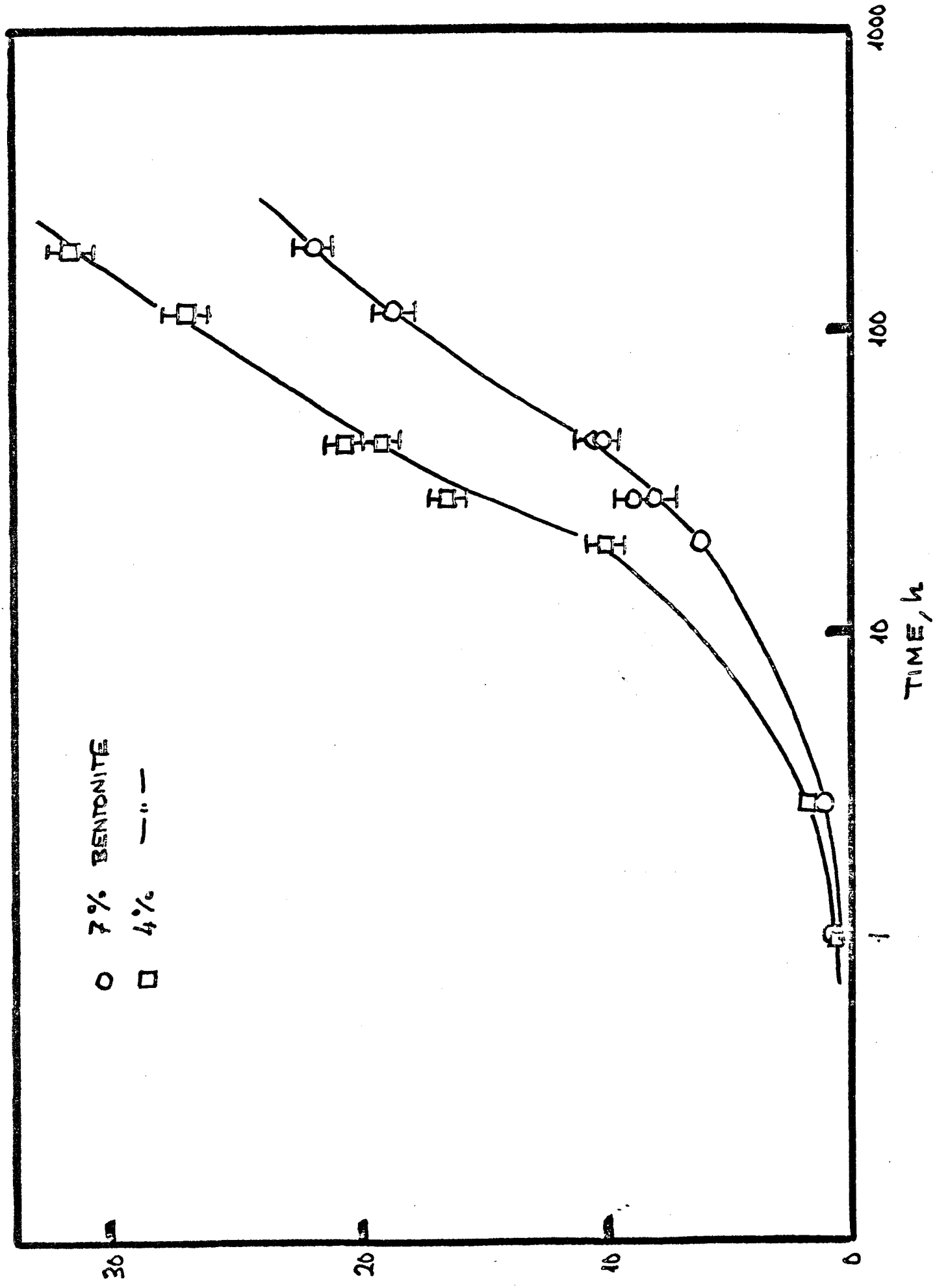

Swelling of bentonite in glass cell

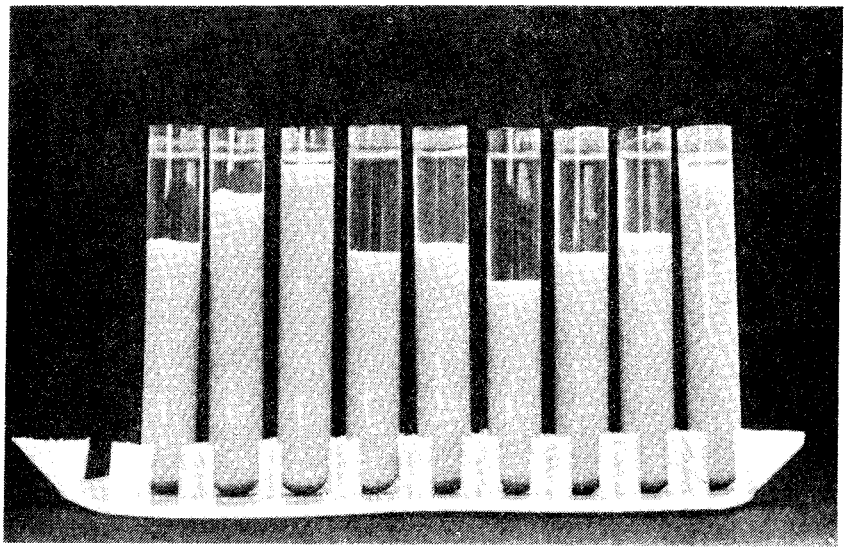

A

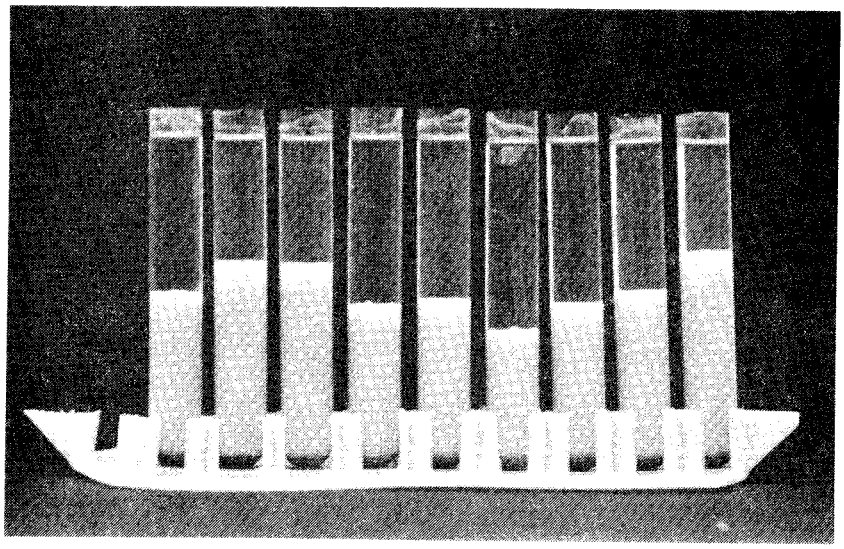

B

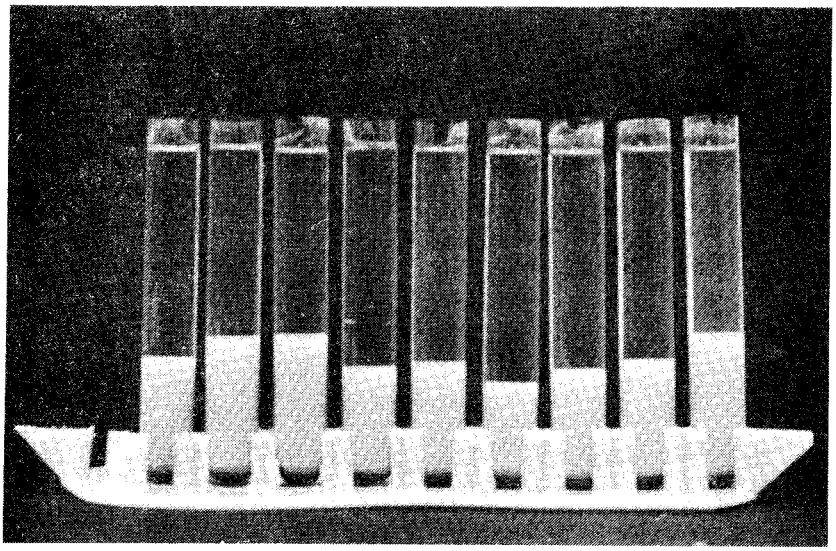

C

Changes in sediment volumes, 5% bentonite in different waters, A 2000RPM - 500x g, B 5000 RPM - 3150x g, C 10000 RPM - 12600x g.

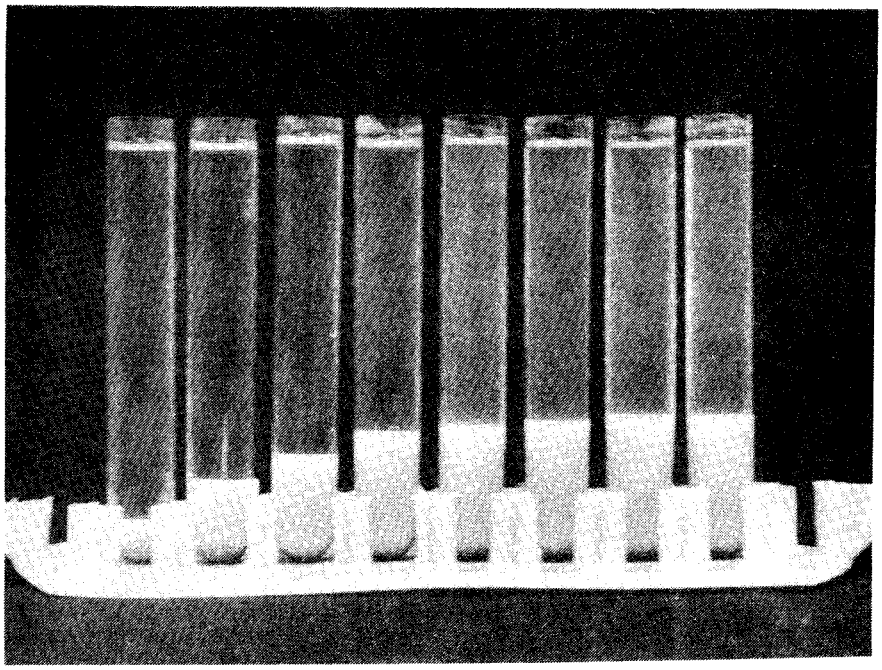

2000 RPM

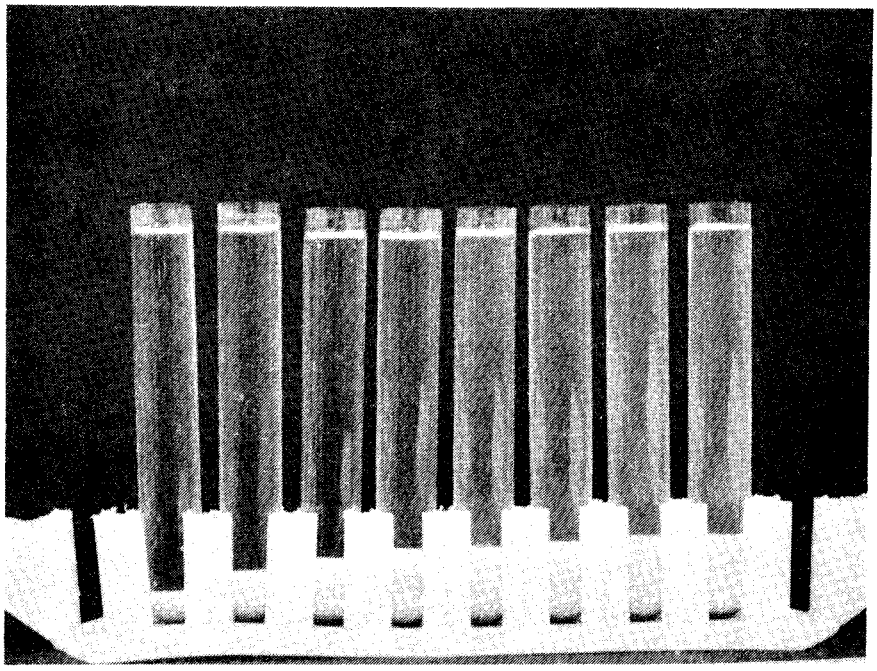

5000 RPM

Sedimentvolumes for centrifugated bentonitegels (2 %).

Ca^{2+}: $5x10^{-3}$, $2x10^{-3}$, $1x10^{-3}$, $5x10^{-4}$, $2x10^{-4}$, $1x10^{-4}$, $1xlo^{-5}$, dist. water, dist. water, from left to right.

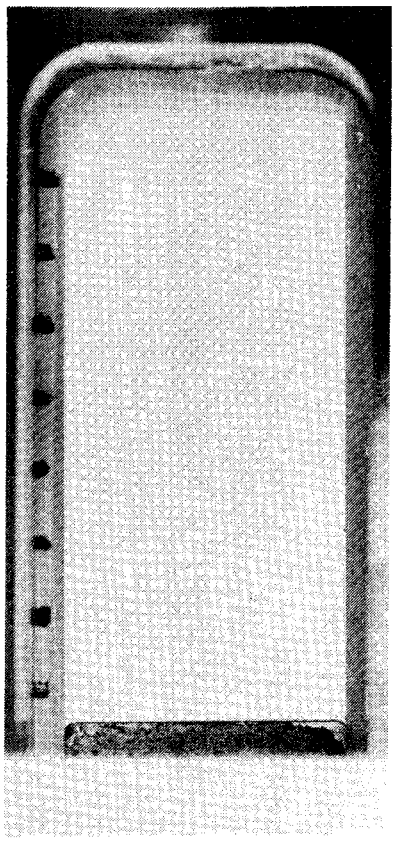

0 min

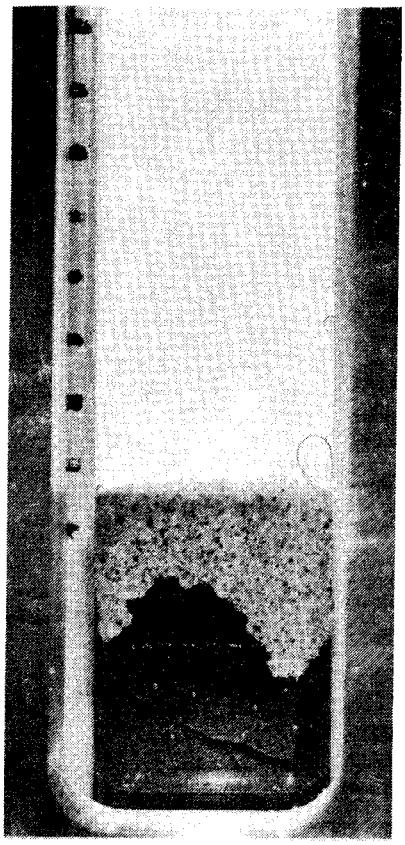

2 min 55 s

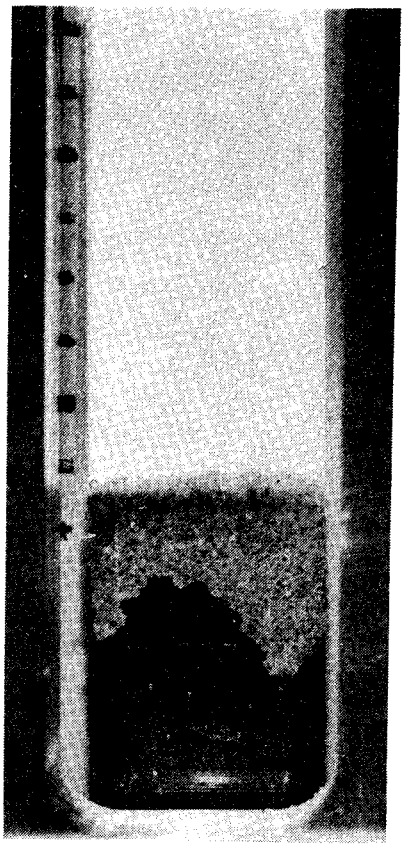

12 min

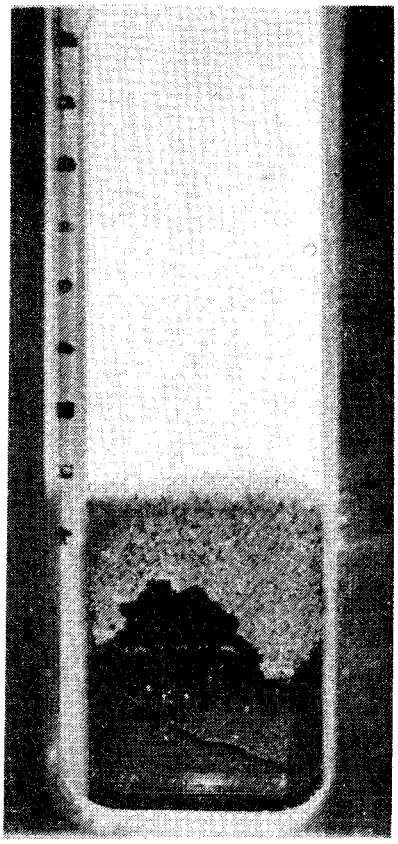

25 min

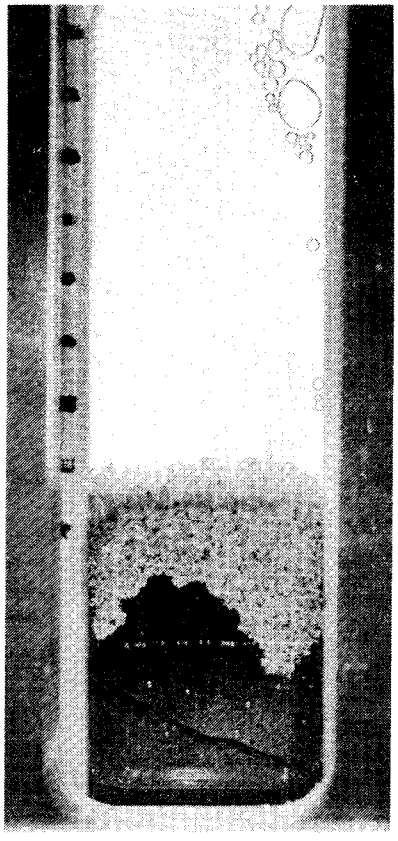

1 h 10 min

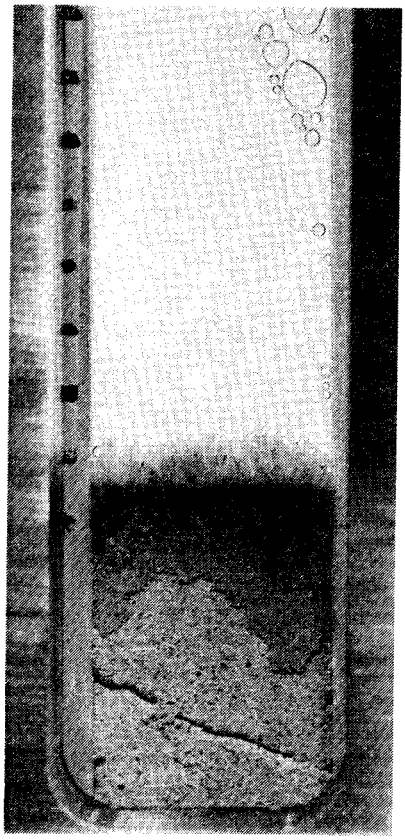

4 h 30 min

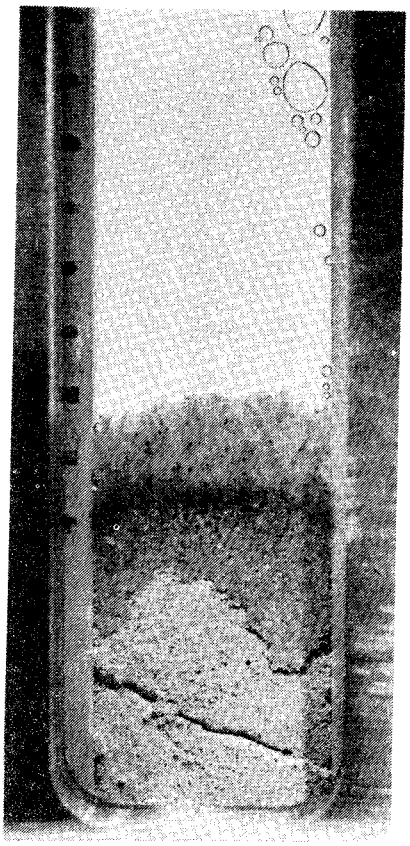

26 h 15 min

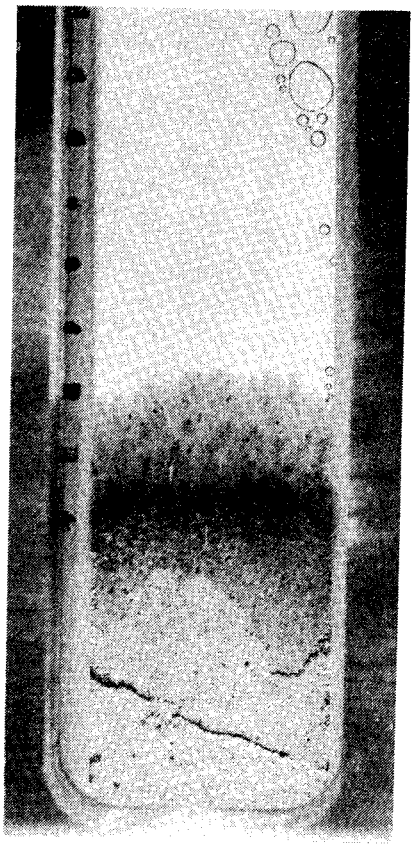

49 h 30 min

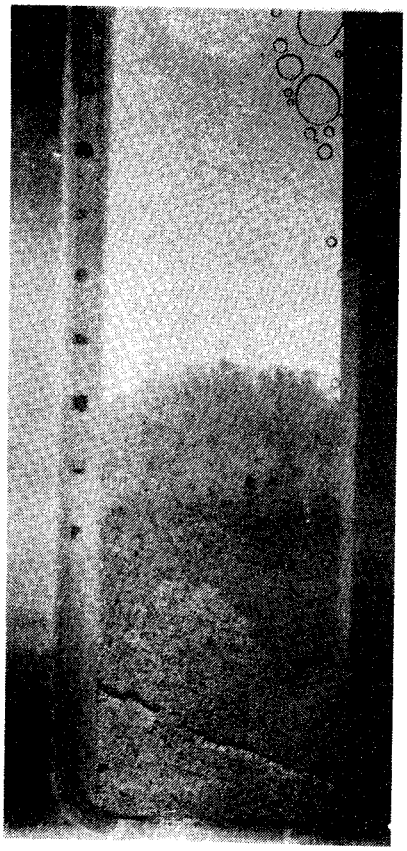

74 h

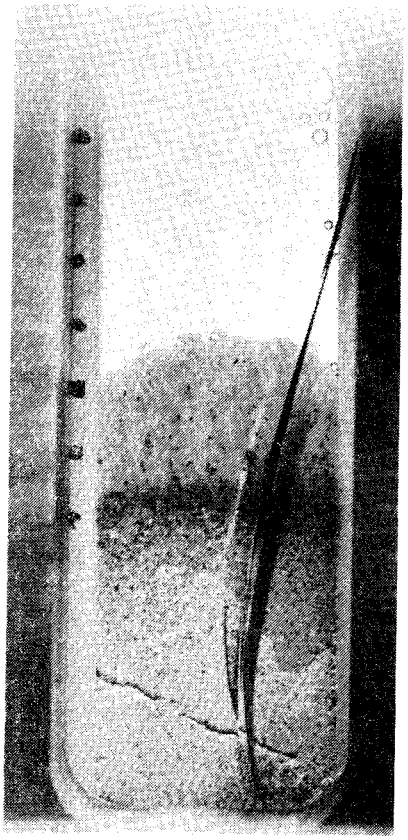

100 h 35 min

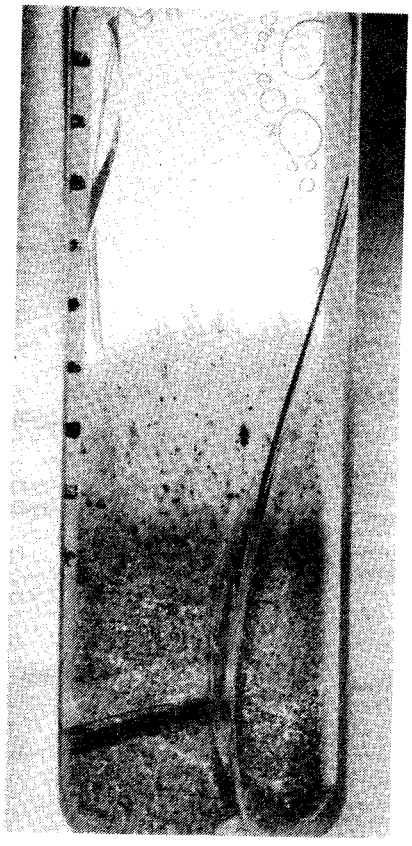

118 h

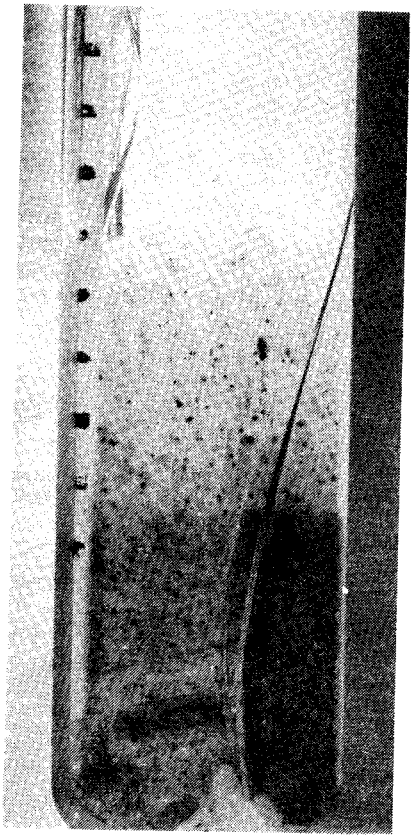

169 h

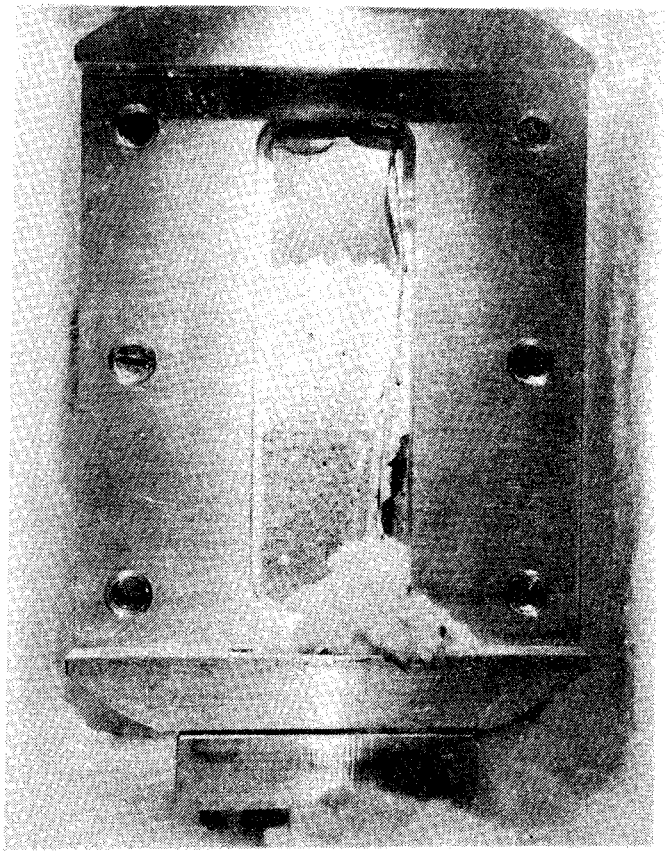

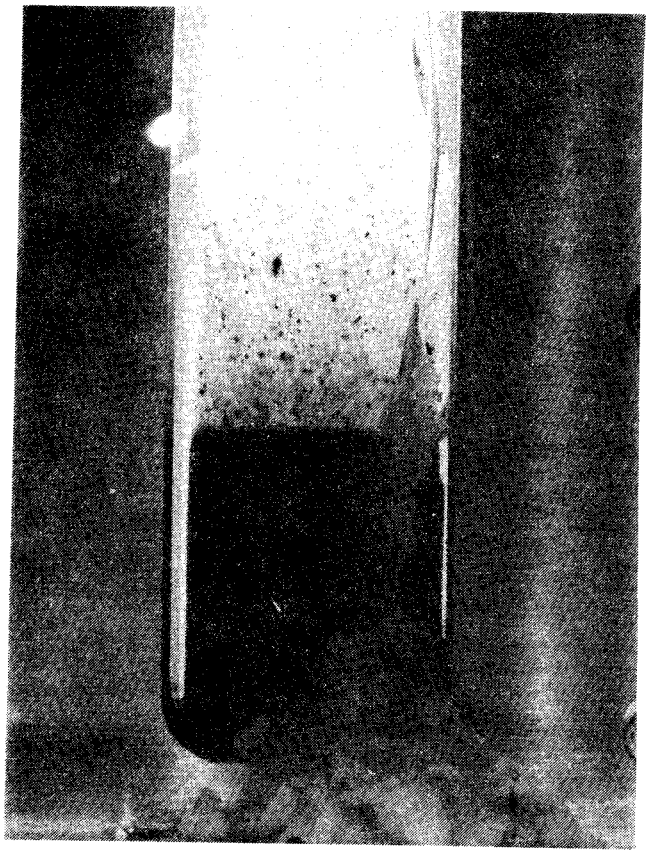

70 hours after crack in the glass cell occurred.

Appendix 2

1. Light scattering measurements

2. Diffusion

1. Light scattering measurements

The particle concentrations were determined by comparing the intensities measured for the bentonite suspensions by comparing them to a standard, monodisperse polystyrene, diam. 330 nm. It should be noted that this method assumes spherical particles and the same optical properties for the sample and the reference which certainly is not the case. Hence, the results should be considered relative, not absolute.

The scattered intensity is given by

$$I = K^{11}\, n\, m^2$$

where

K^{11} = an optical constant

n = refractive index of the scattering material at the wave length λ of the scattered light

m = number of particles per unit volume

For spherical particles with radius r and density ρ this equation can be written

$$I = K\, c r^3 \rho$$

where c is the concentration (mass/unit volume). The measurements are calibrated using a sample with known

$\rho = \rho_{ref}$, concentration c_{ref} and radius r_{ref}

$$I_{ref} = K\, c_{ref}\, r^3_{ref}\, \rho_{ref}$$

The scattered intensity from the sample (concentration c_s) is given by

$$I_s = K\, c_s\, r_s^3\, \rho_s$$

if it is assumed that the particles have the same optical properties as the reference and that they are spherical with radius r_s.

The density of polystyren is 1.05 g/cm^3 and of montmorillonite 2.7 g/cm^3.
The assumption $\rho_{ref} = \rho_s$ gives at least 2 times too high concentrations for the sample. On the other hand, the other assumptions in the equations are also very rough. In any case, the method gives a relative estimate of the particle concentration which is pessimistic and sufficient for the present purpose.

Other constants used for the calculations were:

T = 295 K
η = viscosity of water
λ = 632.8 nm
n = 1.33
$\theta = 40^{o}$

2. Diffusion

1. The diffusion coefficients for calcium were calculated from the average displacement (50)

$$\bar{X} = \sqrt{2Dt}$$

2. For lignosulphonate diffusion the following equation was used (50):

$$D = \frac{s^2 \pi}{q^2 c_o^2 t}$$

where s = total amount diffused across a cylinder cross section
q = during the time t,
c_o = initial concentration, kept constant in the solution

THE SWELLING PRESSURE AND THE EQUILIBRIUM VOLUME OF BENTONITE

1. The disjoining pressure in a thin film

Let us assume that an amount of material, dn, is transferred from a bulk phase to a thin film in contact with this phase (fig. 1). This transfer can be carried out in two steps.

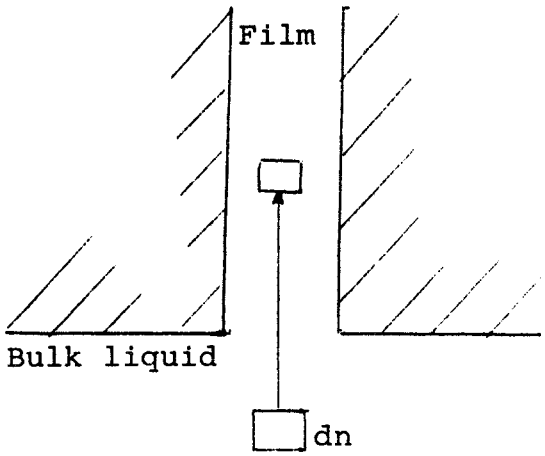

Fig. 1. A thin film of liquid in contact with bulk liquid.

I. The material is transferred from the bulk phase into the film, keeping the state of stress equal to that of the isotropic bulk liquid. In the film, due to the close vicinity to the surfaces, the physico-chemical forces acting on the element are different from those in the bulk phase. Hence, the chemical potential of the element is changed by the amount

$$\Delta \bar{\mu} = \mu_I^f - \mu^b \ (p^b, T) \qquad (1)$$

II. The state of stress in the film is different from that in the bulk. In the second step, hence, the stress on the element is allowed to change from the isotropic pressure p^b in the bulk to the anisotropic volumetric mean stress $\bar{p}^f$. The chemical potential of the element then changes by

$$\mu_{II}^f - \mu_I^f = \int_{p^b}^{\bar{p}^f} \left(\frac{\partial \mu}{\partial p}\right)_T \, dp \qquad (2)$$

If the liquid is assumed to be incompressible,

$$\left(\frac{\partial \mu}{\partial \rho}\right)_T = v \tag{3}$$

where v is the partial molar volume of the liquid. Hence,

$$\mu_{II}{}^f - \mu_I{}^f = (\bar{p}^f - p^b)v \tag{4}$$

If the film is in equilibrium with the bulk liquid,

$$\mu_{II}{}^f = \mu^f(\bar{p}^f, T) = \mu^b(p^b, T) \tag{5}$$

It follows from (1) and (4) that

$$\bar{p}^f - p^b \equiv \pi_D = -\frac{\Delta\bar{\mu}}{v} \tag{6}$$

The difference in stress between the material in the film and the material in the bulk is exactly balanced by the change in chemical potential experienced by the material when it is transferred from the bulk liquid to the film. This difference is usually called the disjoining pressure, π_D. It is often identified with the pressure normal to the film surfaces.

π_D is strongly dependent on the distance h between the film surfaces. This dependence is usually divided into various contributions, those best understood being

- electrostatic pressure due to double layer interactions,
- electromagnetic pressure due to van der Waals interactions,
- pressure due to steric interactions between adsorbed molecules.

In multicomponent systems, adsorption at the surfaces will occur and hence the composition of the film will not necessarily be the same as that of the bulk phase.

2. The swelling pressure of bentonite

The swelling pressure of wet bentonite is due to the disjoining pressure in the thin films of water between the montmorillonite layers. Several studies have been made of this pressure (see fig. 6.6) that indicate that when the clay is not very strongly compressed the double layer interactions are of predominating importance in the clay. As a consequence, the swelling pressure is strongly dependent on the ionic strength and the charge of the cation in the electrolyte between the montmorillonite platelets. At any given external pressure, the clay will swell until the disjoining pressure is equal to this external pressure. Fig. 6.6 gives the distances between the montmorillonite platelets for montmorillonite in equilibrium with bulk solution. The pressure in this bulk solution is 1 atm. Thus we may read from the curve for 10^{-3} mol dm^{-3} $MgSO_4$ that to maintain an equilibrium distance of 1 nm between the platelets,a pressure of about 50 atm is needed on the montmorillonite if it is to be in equilibrium with 10^{-3} mol dm^{-3} $MgSO_4$ at 1 atm. If allowed to swell freely in this solution, the clay will increase its volume until the plate-to-plate distance is about 2.2 nm; the disjoining pressure then is 1 atm.

It is interesting to discuss the effect of increasing the pressure on the bulk liquid. The change in chemical potential with pressure is given by eq. (3), i.e. the chemical potential is increased. If the pressure is increased to, say, 50 atm, the clay if allowed to swell freely will now, of course, swell until the disjoining pressure is 50 atm. The equilibrium distance between the platelets, again, will be determined by the condition that the chemical potentials of the liquid must be equal in the bulk and in the clay.

If the molar volumes of the liquid are equal in the clay and in the bulk liquid, the chemical potentials change at the same rate in both systems. To maintain a given equilibrium distance, hence, $\bar{p}^f - p^b$ should be kept constant. As a very important special case it can be concluded that if the clay is allowed to swell freely in contact with an electrolyte solution (i.e., until $\bar{p}^f - p^b = 0$), increasing the pressure on both clay and liquid will not change the equilibrium distance. To predict the exact behaviour of real bentonite one would need to know the partial molar volumes of the components in the bulk and in the liquid between the platelets. However, the assumption that they are roughly equal is certainly good enough for the present purpose.

3. Conclusions of importance to the swelling behaviour of the confined bentonite

1. If the bentonite is kept in contact with ground water and its volume is allowed to increase freely, it will eventually swell until the pressure in the clay and the pressure in the ground water are equal, i.e. the swelling pressure is zero. If 10^{-3} mol dm^{-3} $MgSO_4$ can be taken as model ground water for this purpose, fig 6.6 indicates that the distance between the plates will be 1.5-2 nm corresponding to an increase in volume of about 60-100%. It should be stressed, however, that this equilibrium situation may be reached extremely slowly due to the slow diffusion of water into the gel.

2. An obvious way to prevent or limit this swelling is to maintain a sufficiently large pressure difference between the clay and the surrounding ground water.

FÖRTECKNING ÖVER KBS TEKNISKA RAPPORTER

01 Källstyrkor i utbränt bränsle och högaktivt avfall från en PWR beräknade med ORIGEN
Nils Kjellbert
AB Atomenergi 77-04-05

02 PM angående värmeledningstal hos jordmaterial
Sven Knutsson
Roland Pusch
Högskolan i Luleå 77-04-15

03 Deponering av högaktivt avfall i borrhål med buffertsubstans
Arvid Jacobsson
Roland Pusch
Högskolan i Luleå 77-05-27

04 Deponering av högaktivt avfall i tunnlar med buffertsubstans
Arvid Jacobsson
Roland Pusch
Högskolan i Luleå 77-06-01

05 Orienterande temperaturberäkningar för slutförvaring i berg av radioaktivt avfall, Rapport 1
Roland Blomqvist
AB Atomenergi 77-03-17

06 Groundwater movements around a repository, Phase 1, State of the art and detailed study plan
Ulf Lindblom
Hagconsult AB 77-02-28

07 Resteffekt studier för KBS
Del 1 Litteraturgenomgång
Del 2 Beräkningar
Kim Ekberg
Nils Kjellbert
Göran Olsson
AB Atomenergi 77-04-19

08 Utlakning av franskt, engelskt och kanadensiskt glas med högaktivt avfall
Göran Blomqvist
AB Atomenergi 77-05-20

09 Diffusion of soluble materials in a fluid filling a porous medium
Hans Häggblom
AB Atomenergi 77-03-24

10 Translation and development of the BNWL-Geosphere Model
Bertil Grundfelt
Kemakta Konsult AB 77-02-05

11 Utredning rörande titans lämplighet som korrosionshärdig kapsling för kärnbränsleavfall
Sture Henriksson
AB Atomenergi 77-04-18

12 Bedömning av egenskaper och funktion hos betong i samband med slutlig förvaring av kärnbränsleavfall i berg
Sven G Bergström
Göran Fagerlund
Lars Rombén
Cement- och Betonginstitutet 77-06-22

13 Urlakning av använt kärnbränsle (bestrålad uranoxid) vid direktdeponering
Ragnar Gelin
AB Atomenergi 77-06-08

14 Influence of cementation on the deformation properties of bentonite/quartz buffer substance
Roland Pusch
Högskolan i Luleå 77-06-20

15 Orienterande temperaturberäkningar för slutförvaring i berg av radioaktivt avfall
Rapport 2
Roland Blomquist
AB Atomenergi 77-05-17

16 Översikt av utländska riskanalyser samt planer och projekt rörande slutförvaring
Åke Hultgren
AB Atomenergi augusti 1977

17 The gravity field in Fennoscandia and postglacial crustal movements
Arne Bjerhammar
Stockholm augusti 1977

18 Rörelser och instabilitet i den svenska berggrunden
Nils-Axel Mörner
Stockholms Universitet augusti 1977

19 Studier av neotektonisk aktivitet i mellersta och norra Sverige, flygbildsgenomgång och geofysisk tolkning av recenta förkastningar
Robert Lagerbäck
Herbert Henkel
Sveriges Geologiska Undersökning september 1977

20 Tektonisk analys av södra Sverige, Vättern - Norra Skåne
Kennert Röshoff
Erik Lagerlund
Lunds Universitet och Högskolan Luleå september 1977

21 Earthquakes of Sweden 1891 - 1957, 1963 - 1972
Ota Kulhánek
Rutger Wahlström
Uppsala Universitet september 1977

22 The influence of rock movement on the stress/strain situation in tunnels or bore holes with radioactive consisters embedded in a bentonite/quartz buffer mass
Roland Pusch
Högskolan i Luleå 1977-08-22

23 Water uptake in a bentonite buffer mass
A model study
Roland Pusch
Högskolan i Luleå 1977-08-22

24 Beräkning av utlakning av vissa fissionsprodukter och aktinider från en cylinder av franskt glas
Göran Blomqvist
AB Atomenergi 1977-07-27

25 Blekinge kustgnejs, Geologi och hydrogeologi
Ingemar Larsson KTH
Tom Lundgren SGI
Ulf Wiklander SGU
Stockholm, augusti 1977

26 Bedömning av risken för fördröjt brott i titan
Kjell Pettersson
AB Atomenergi 1977-08-25

27 A short review of the formation, stability and cementing properties of natural zeolites
Arvid Jacobsson
Högskolan i Luleå 1977-10-03

28 Värmeledningsförsök på buffertsubstans av bentonit/pitesilt
Sven Knutsson
Högskolan i Luleå 1977-09-20

29 Deformationer i sprickigt berg
Ove Stephansson
Högskolan i Luleå 1977-09-28

30 Retardation of escaping nuclides from a final depository
Ivars Neretnieks
Kungliga Tekniska Högskolan Stockholm 1977-09-14

31 Bedömning av korrosionsbeständigheten hos material avsedda för kapsling av kärnbränsleavfall. Lägesrapport 1977-09-27 samt kompletterande yttranden.
Korrosionsinstitutet och dess referensgrupp

32 Long term mineralogical properties of bentonite/quartz buffer substance
Preliminär rapport november 1977
Slutrapport februari 1978
Roland Pusch
Arvid Jacobsson
Högskolan i Luleå

33 Required physical and mechanical properties of buffer masses
Roland Pusch
Högskolan Luleå 1977-10-19

34 Tillverkning av bly-titan kapsel
Folke Sandelin AB
VBB
ASEA-Kabel
Institutet för metallforskning
Stockholm november 1977

35 Project for the handling and storage of vitrified high-level waste
Saint Gobain Techniques Nouvelles October, 1977

36 Sammansättning av grundvatten på större djup i granitisk berggrund
Jan Rennerfelt
Orrje & Co, Stockholm 1977-11-07

37 Hantering av buffertmaterial av bentonit och kvarts
Hans Fagerström, VBB
Björn Lundahl, Stabilator
Stockholm oktober 1977

38 Utformning av bergrumsanläggningar
Arne Finné, KBS
Alf Engelbrektson, VBB
Stockholm december 1977

39 Konstruktionsstudier, direktdeponering
ASEA-ATOM
VBB
Västerås

40 Ekologisk transport och stråldoser från grundvattenburna radioaktiva ämnen
Ronny Bergman
Ulla Bergström
Sverker Evans
AB Atomenergi

41 Säkerhet och strålskydd inom kärnkraftområdet.
Lagar, normer och bedömningsgrunder
Christina Gyllander
Siegfried F Johnson
Stig Rolandson
AB Atomenergi och ASEA-ATOM

42 Säkerhet vid hantering, lagring och transport av använt kärnbränsle och förglasat högaktivt avfall
Ann Margret Ericsson
Kemakta november 1977

43 Transport av radioaktiva ämnen med grundvatten från ett bergförvar
Bertil Grundfelt
Kemakta november 1977

44 Beständighet hos borsilikatglas
Tibor Lakatos
Glasteknisk Utveckling AB

45 Beräkning av temperaturer i ett envånings slutförvar i berg för förglasat radioaktivt avfall Rapport 3
Roland Blomquist
AB Atomenergi 1977-10-19

46 Temperaturberäkningar för använt bränsle
Taivo Tarandi
VBB

47 Teoretiska studier av grundvattenrörelser
Preliminär rapport oktober 1977
Slutrapport februari 1978
Lars Y Nilsson
John Stokes
Roger Thunvik
Inst för kulturteknik KTH

48 The mechanical properties of the rocks in Stripa, Kråkemåla, Finnsjön and Blekinge
Graham Swan
Högskolan i Luleå 1977-09-14

49 Bergspänningsmätningar i Stripa gruva
Hans Carlsson
Högskolan i Luleå 1977-08-29

50 Lakningsförsök med högaktivt franskt glas i Studsvik
Göran Blomqvist
AB Atomenergi november 1977

51 Seismotechtonic risk modelling for nuclear waste disposal in the Swedish bedrock
F Ringdal
H Gjöystdal
E S Hysebye
Royal Norwegian Council for scientific and industrial research

52 Calculations of nuclide migration in rock and porous media, penetrated by water
H Häggblom
AB Atomenergi 1977-09-14

53 Mätning av diffusionshastighet för silver i lera-sand-blandning
Bert Allard
Heino Kipatsi
Chalmers tekniska högskola 1977-10-15

54 Groundwater movements around a repository

54:01 Geological and geotechnical conditions
Håkan Stille
Anthony Burgess
Ulf E Lindblom
Hagconsult AB september 1977

54:02 Thermal analyses
Part 1 Conduction heat transfer
Part 2 Advective heat transfer
Joe L Ratigan
Hagconsult AB september 1977

54:03 Regional groundwater flow analyses
Part 1 Initial conditions
Part 2 Long term residual conditions
Anthony Burgess
Hagconsult AB oktober 1977

54:04 Rock mechanics analyses
Joe L Ratigan
Hagconsult AB september 1977

54:05 Repository domain groundwater flow analyses
Part 1 Permeability perturbations
Part 2 Inflow to repository
Part 3 Thermally induced flow
Joe L Ratigan
Anthony S Burgess
Edward L Skiba
Robin Charlwood

54:06 Final report
Ulf Lindblom et al
Hagconsult AB oktober 1977

55 Sorption av långlivade radionuklider i lera och berg
Del 1 Bestämning av fördelningskoefficienter
Del 2 Litteraturgenomgång
Bert Allard
Heino Kipatsi
Jan Rydberg
Chalmers tekniska högskola 1977-10-10

56 Radiolys av utfyllnadsmaterial
Bert Allard
Heino Kipatsi
Jan Rydberg
Chalmers tkniska högskola 1977-10-15

57 Stråldoser vid haveri under sjötransport av kärnbränsle
Anders Appelgren
Ulla Bergström
Lennart Devell
AB Atomenergi 1978-01-09

58 Strålrisker och högsta tillåtliga stråldoser för människan
Gunnar Walinder
FOA 4 november 1977

59 Tectonic lineaments in the Baltic from Gävle to Simrishamn
Tom Flodén
Stockholms Universitet 1977-12-15

60 Förarbeten för platsval, berggrundsundersökningar
Sören Scherman

Berggrundvattenförhållande i Finnsjöområdets nordöstra del
Carl-Erik Klockars
Ove Persson
Sveriges Geologiska Undersökning januari 1978

61 Permeabilitetsbestämningar
Anders Hult
Gunnar Gidlund
Ulf Thoregren

Geofysisk borrhålsmätning
Kurt-Åke Magnusson
Oscar Duran
Sveriges Geologiska Undersökning januari 1978

62 Analyser och åldersbestämningar av grundvatten på stora djup
Gunnar Gidlund
Sveriges Geologiska Undersökning 1978-02-14

63 Geologisk och hydrogeologisk grunddokumentation av
Stripa försöksstation
Andrei Olkiewicz
Kenth Hansson
Karl-Erik Almén
Gunnar Gidlund
Sveriges Geologiska Undersökning februari 1978

64 Spänningsmätningar i Skandinavisk berggrund - förutsättningar, resultat och tolkning
Sten G A Bergman
Stockholm november 1977

65 Säkerhetsanalys av inkapslingsprocesser
Göran Carleson
AB Atomenergi 1978-01-27

66 Några synpunkter på mekanisk säkerhet hos kapsel för kärnbränsleavfall
Fred Nilsson
Kungl Tekniska Högskolan Stockholm februari 1978

67 Mätning av galvanisk korrosion mellan titan och bly samt mätning av titans korrosionspotential under γ- bestrålning. 3 st tekniska PM.
Sture Henrikson
Stefan Poturaj
Maths Åsberg
Derek Lewis
AB Atomenergi januari-februari 1978

68 Degraderingsmekanismer vid bassänglagring och hantering av utbränt kraftreaktorbränsle
Gunnar Vesterlund
Torsten Olsson
ASEA-ATOM 1978-01-18

69 A three-dimensional method for calculating the hydraulic gradient in porous and cracked media
Hans Häggblom
AB Atomenergi 1978-01-26

70 Lakning av bestrålat UO_2-bränsle
Ulla-Britt Eklund
Ronald Forsyth
AB Atomenergi 1978-02-24

71 Bergspricktätning med bentonit
Roland Pusch
Högskolan i Luleå 1977-11-16

72 Värmeledningsförsök på buffertsubstans av kompakterad bentonit
Sven Knutsson
Högskolan i Luleå 1977-11-18

73 Self-injection of highly compacted bentonite into rock joints
Roland Pusch
Högskolan i Luleå 1978-02-25

74 Highly compacted Na bentonite as buffer substance
Roland Pusch
Högskolan i Luleå 1978-02-25

75 Small-scale bentonite injection test on rock
Roland Pusch
Högskolan i Luleå 1978-03-02

76 Experimental determination of the stress/strain situation in a sheared tunnel model with canister
Roland Pusch
Högskolan i Luleå 1978-03-02

77 Nuklidvandring från ett bergförvar för utbränt bränsle
Bertil Grundfelt
Kemakta konsult AB, Stockholm

78 Bedömning av radiolys i grundvatten
Hilbert Christenssen
AB Atomenergi 1978-02-17

79 Transport of oxidants and radionuclides through a clay barrier
Ivars Neretnieks
Kungl Tekniska Högskolan Stockholm 1978-02-20

80 Utdiffusion av svårlösliga nuklider ur kapsel efter kapselgenombrott
Karin Andersson
Ivars Neretnieks
Kungl Tekniska Högskolan Stockholm 1978-03-07

81 Tillverkning av kopparkapsel
Kåre Hannerz
Stefan Sehlstedt
Bengt Lönnerberg
Liberth Karlson
Gunnar Nilsson
ASEA, ASEA-ATOM

82 Hantering och slutförvaring av aktiva metalldelar
Bengt Lönnerberg
Alf Engelbrektsson
Ivars Neretnieks
ASEA-ATOM, VBB, KTH

83 Hantering av kapslar med använt bränsle i slutförvaret
Alf Engelbrektsson
VBB Stockholm april 1978

84 Tillverkning och hantering av bentonitblock
Alf Engelbrektsson
Ulf Odebo
ASEA, VBB

85 Beräkning av kryphastigheten hos ett blyhölje innehållande en glaskropp under inverkan av tyngdkraften
Anders Samuelsson

Förändring av krypegenskaperna hos ett blyhölje som följd av en mekanisk skada
Göran Eklund
Institutet för Metallforskning september 1977 - april 1978

86 Diffusivitetsmätningar av metan och väte i våt lera
Ivars Neretnieks
Christina Skagius
Kungl Tekniska Högskolan Stockholm 1978-01-09

87 Diffusivitetsmätningar i våt lera Na-lignosulfonat, Sr^{2+}, Cs^{+}
Ivars Neretnieks
Christina Skagius
Kungl Tekniska Högskolan Stockholm 1978-03-16

88 Ground water chemistry at depth in granites and gneisses
Gunnar Jacks
Kungl Tekniska Högskolan Stockholm april 1978

89 Inverkan av glaciation på en deponeringsanläggning belägen i urberg 500 m under markytan
Roland Pusch
Högskolan i Luleå 1978-03-16

90 Koppar som kapslingsmaterial för icke upparbetat kärnbränsleavfall - bedömning ur korrosionssynpunkt
Lägesrapport 1978-03-31
Korrosionsinstitutet och dess referensgrupp

91 Korttidsvariationer i grundvattnets trycknivå
Lars Y Nilsson
Kungliga Tekniska Högskolan Stockholm september 1977

92 Termisk utvidgning hos granitoida bergarter
Ove Stephansson
Högskolan i Luleå april 1978

93 Preliminary corrosion studies of glass ceramic code 9617 and a sealing frit for nuclear waste canisters
I D Sundquist
Corning Glass Works 78-03-14

94 Avfallsströmmar i upparbetningsprocessen
Birgitta Andersson
Ann-Margret Ericsson
Kemakta mars 1978

95 Separering av C-14 vid upparbetningsprocessen
Sven Brandberg
Ann-Margret Ericsson
Kemakta mars 1978

96 Korrosionsprovning av olegerat titan i simulerade deponeringsmiljöer för upparbetat kärnbränsleeavfall
Sture Henrikson
Marian de Pourbaix
AB Atomenergi 1978-04-24

97 Colloid chemical aspects of the "confined bentonite concept"
Jean C Le Bell
Ytkemiska Institutet 1978-03-07

98 Sorption av långlivade radionuklider i lera och berg Del 2
Bert Allard
Heino Kipatsi
Börje Torstenfelt
Chalmers Tekniska Högskola 1978-04-20